Deep-sea Research Part Ii-topical Studies In Oceanography
March 2015, Volume 113 Pages 125-144
https://doi.org/10.1016/j.dsr2.2014.10.026
https://archimer.ifremer.fr/doc/00226/33762/

Archimer
https://archimer.ifremer.fr

Seasonal oceanography from Physics to micronekton in the south-west pacific

Menkes C. E. [1], Allain V. [2,] *, Rodier M. [3], Gallois F. [4], Lebourges-Dhaussy A. [5], Hunt B. P. V. [6, 7], Smeti H. [1, 6, 8], Pagano M. [6], Josse E. [5], Daroux A. [5], Lehodey P. [9], Senina I. [9], Kestenare E. [10], Lorrain A. [11], Nicol S. [2]

[1] Univ Paris 06, Univ Paris 04, Inst Rech & Dev, CNRS MNHN,LOCEAN Lab,IRD Noumea, Noumea 98848, New Caledonia.
[2] Secretariat Pacific Community, Noumea 98848, New Caledonia.
[3] IRD Tahiti, IRD UMR 241, Inst Rech & Dev, Papeete 98713, Tahiti, Fr Polynesia.
[4] IRD Noumea, Inst Rech & Dev, IRD US IMAGO 199, Noumea 98848, New Caledonia.
[5] LEMAR UMR6539, F-29280 Plouzane, France.
[6] Univ Toulon & Var, Aix Marseille Univ, Mediterranean Inst Oceanog, CNRS,IRD,MIO UM 110, F-13288 Marseille, France.
[7] Univ British Columbia, Dept Earth Ocean & Atmospher Sci, Vancouver, BC V6T 1Z4, Canada.
[8] Natl Inst Marine Sci INSTM, Salammbo, Tunisia.
[9] CLS, F-31520 Ramonville St Agne, France.
[10] IRD UMR LEGOS OMP 5566, Inst Rech & Dev, F-31400 Toulouse, France.
[11] IRD Noumea, Inst Rech & Dev, IRD LEMAR R195, Noumea 98848, New Caledonia.

* Corresponding author : C. E. Menkes, email address : christophe.menkes@ird.fr

valeriea@spc.int ; martine.rodier@ird.fr ; francis.gallois@ird.fr ; Anne.Lebourges.Dhaussy@ird.fr ; bhunt@eos.ubc.ca ; houssem.smeti@gmail.com ; marc.pagano@ird.fr ; Erwan.Josse@ird.fr ; aurelie.daroux@hotmail.fr ; plehodey@cls.fr ; inna.senina@gmail.com ; Elodie.kestenare@ird.fr ; anne.lorrain@ird.fr ; simonn@spc.int

Abstract :

Tuna catches represent a major economic and food source in the Pacific Ocean, yet are highly variable. This variability in tuna catches remains poorly explained. The relationships between the distributions of tuna and their forage (micronekton) have been mostly derived from model estimates. Observations of micronekton and other mid-trophic level organisms, and their link to regional oceanography, however are scarce and constitute an important gap in our knowledge and understanding of the dynamics of pelagic ecosystems. To fill this gap, we conducted two multidisciplinary cruises (Nectalis1 and Nectalis2) in the New Caledonian Exclusive Economic Zone (EEZ) at the southeastern edge the Coral Sea, in 2011 to characterize the oceanography of the region during the cool (August) and the hot (December) seasons. The physical and biological environments were described by hydrology, nutrients and phytoplankton size structure and biomass. Zooplankton biomass was estimated from net sampling and acoustics and micronecton was estimated from net sampling, the SEAPODYM ecosystem model, a dedicated echosounder and non-dedicated acoustics. Results demonstrated that New Caledonia is located in an

Please note that this is an author-produced PDF of an article accepted for publication following peer review. The definitive publisher-authenticated version is available on the publisher Web site.

oligotrophic area characterized by low nutrient and low primary production which is dominated by a high percentage of picoplankton cyanobacteria Prochlorococcus (>90%). The area is characterized by a large-scale north-south temperature and salinity gradient. The northern area is influenced by the equatorial Warm Pool and the South Pacific Convergence Zone and is characterized by higher temperature, lower salinity, lower primary production and micronekton biomass. The southern area is influenced by the Tasman Sea and is characterized by cooler temperature, higher salinity, higher primary production and micronekton biomass. Interactions between the dynamic oceanography and the complex topography creates a myriad of mesoscale eddies, inducing patchy structures in the frontal area. During the cool season, a tight coupling existed between the ocean dynamics and primary production, while there was a stronger decoupling during the hot season. There was little difference in the composition of mid-trophic level organisms (zooplankton and micronekton) between the two seasons. This may be due to different turn-over times and delays in the transmission of primary production to upper trophic levels. Examination of various sampling gears for zooplankton and micronekton showed that net biomass estimates and acoustic-derived estimates compared reasonably well. Estimates of micronekton from net observations and the SEAPODYM model were in the same range. The non-dedicated acoustics adequately reproduced trends observed in zooplankton from nets, but the acoustics could not differentiate between zooplankton and micronekton and absolute biomasses could not be calculated. Understanding the impact of mesoscale features on higher trophic levels will require further investigation and patchiness induced by eddies raises the question of how to best sample highly dynamic areas via sea experiments.

Keywords : Zooplankton, Nekton, Acoustic data, Oceanographic surveys, Mesoscale eddies, Oligotrophic, Primary production

Please note that this is an author-produced PDF of an article accepted for publication following peer review. The definitive publisher-authenticated version is available on the publisher Web site.

1 Introduction

In the South Pacific Ocean fishing of apex predators, such as tuna and billfishes, represents a major economic and food resource (Bell et al., 2013). Considerable variability in tuna catch rates is observed in fisheries (Rouyer et al., 2008). Although much of this variability remains unexplained, tuna abundance in space and time has been correlated with factors including oceanographic conditions, physiological constraints (*e.g.* temperature, depth, oxygen requirements), forage availability, and reproductive behavior (Farley et al., 2013; Senina et al., 2008; Young et al., 2011).

Tuna forage predominantly comprises micronekton (Young et al., 2010; this issue). Micronekton are defined as organisms in the 2-20 cm size range and are predominantly distributed in the upper 1000 m of the water column. Micronekton play a key role as intermediaries between plankton production, their prey, and top predators. Since micronekton biomass is dependent on the availability of plankton prey, it is expected that plankton production, its oceanographic drivers, and micronekton biomass would be tightly coupled, and therefore act in concert in determining top predator distributions.

The New Caledonian Exclusive Economic Zone (EEZ), a region of more than 1.4 10^6 km², is located in the Coral Sea, at the southeastern edge of the South Pacific (Figure 1). The dominant feature of circulation across 0-150 m is the westward-flowing South Equatorial Current (SEC) from ~25°S to the equator. The SEC flow bifurcates at the Australian continental margin (Ridgway and Dunn, 2003) at ~15°S, with one branch connecting with the southward flowing East Australian Current (EAC) (Qu and Lindstrom, 2002) and the other forming the Gulf of Papua Current which flows northward along the coast of Queensland. Within the Coral Sea, the SEC comprises narrow filaments and jets created by the complex island, reef, seamounts and ridge topography (Gourdeau et al., 2008) namely the North Vanuatu Jet at around 13-15°S, and the North Caledonian Jet at around 17-18°S (Couvelard et al., 2008; Marchesiello et al., 2010). To the south of New Caledonia, the surface flow returns from the EAC back into the central south Pacific (Figure 1) as the South Tropical Counter Current (STCC) (Marchesiello et al., 2010). In this region, the structures of the ocean currents are prone to shear instabilities and high eddy kinetic energy is observed

Accepted manuscript

(Qiu et al., 2009). Excluding the very coastal areas, the New Caledonian EEZ is regarded as oligotrophic (Dandonneau and Gohin, 1984) with a mean nitracline depth of ~110 m (Figure 1). South of 22°S, the region experiences higher productivity (Ceccarelli et al., 2013; Dandonneau and Gohin, 1984).

Within this oceanographic context, the longline fishery for tuna represents approximately 30% of the total fisheries harvest in New Caledonia (Gillett, 2009). Catches are dominated by albacore tuna (*Thunnus alalunga*) and exhibit two seasonal peaks in July - August and December, and the highest catch rates occur in the north-western part of the EEZ (Briand et al., 2011). The influence of temperature, primary production and micronekton density on tuna catch rates has been demonstrated in New Caledonia (Briand et al., 2011), in American Samoa (Domokos, 2009) and at the ocean basin scale in the Pacific Ocean (Lehodey et al., 1998).

Large-scale observations of temperature, surface currents and surface primary production derived from satellite data have allowed validation of the existing oceanographic models, giving confidence in the use of modeled oceanographic parameters for such analyses. However there are few observations of biological parameters, including micronekton, to validate the model biological outputs.

At the scale of the South Pacific, nutrient and *in situ* phytoplankton data are sparse, as are data on zooplankton (Carassou et al., 2010; Le Borgne et al., 2011; McKinnon, 2005; Young et al., 2011). Knowledge of the micronektonic communities and their distributions is somewhat more comprehensive, but is based primarily on top predator diet studies (Allain et al., 2012; Olson et al., 2014; Young et al., 2011, 2010). Few data are available from *in situ* sampling with nets in the South Pacific (Flynn and Paxton, 2012; McPherson, 1991) and in general, none of the available micronekton data are coupled with information on oceanographic conditions. These constitute important gaps in our knowledge and understanding of the dynamics of the pelagic ecosystem.

Prior to this study, *in situ* data on micronekton in the New Caledonian region were derived from a handful of studies conducted in the eastern part of the EEZ (Grandperrin, 1975,

Accepted manuscript

ACCEPTED MANUSCRIPT

1969; Legand et al., 1970; Roger, 1986, 1974). Overall, data from the New Caledonia region are limited in both space and time, prohibiting a comprehensive description of the pelagic ecosystem, including the main seasonal patterns of zooplankton and micronekton and their relationships with the oceanography.

In 2011, we conducted two dedicated multi-disciplinary bio-oceanographic cruises (Nectalis1 and Nectalis2) in an effort to fill some knowledge gaps highlighted above for the New Caledonian and greater South Pacific region. Oceanography, nutrient and food web components were sampled in areas of high (north-west) and low (north-east) albacore tuna catch rates in the New Caledonia EEZ, during the austral cool and hot seasons when oceanography is contrasted and tuna catches high. The primary aim of these cruises was to provide insights into how phytoplankton, zooplankton and micronekton are coupled with ocean dynamics in the upper water column (0-1000 m). Here we describe the overall structure of the food web using *in situ* measurements of hydrodynamic parameters, nutrients, phytoplankton distribution, primary production, and the biomass of zooplankton and micronekton. We pay particular attention to the inter-comparability of the zooplankton and micronekton sampling techniques (nets and acoustics) used, and the application of acoustic techniques to improve estimates of micronekton in the future. We also use the collected data to assess measures of micronekton estimated using the ecosystem model SEAPODYM (Lehodey et al., 2010). Finally we interpret our findings in the context of the broader southwest Pacific.

Accepted manuscript

2 Methods and data

Two scientific cruises, Nectalis 1 and 2 were conducted onboard the R/V Alis from 29 July to 16 August 2011 (austral cool season - 18 sampling stations) and 26 November to 14 December 2011 (austral hot season - 23 sampling stations) within the New Caledonian EEZ (Figure 2 and 3). The two cruises were conducted on approximately the same track, with some differences due to weather conditions. The potential spatial variability introduced by variability in station positions between cruises was considered minimal in view of the

ACCEPTED MANUSCRIPT

variability of this highly dynamic pelagic system. Details of station sampling and continuous measurements are summarized in Table 1 and detailed below. Comparisons of ensuing data made between cruises included all stations.

2.1 Data collected during the cruises

2.1.1 **S-ADCP currents**

Five minute averaged ocean currents were acquired from 8 m bins across 16 to 200 m depth using a ship-borne 153 kHz Acoustic Doppler Current Profiler (ADCP – Teledyne RD Instrument, Seattle, USA). These velocity profiles were edited and processed using the CODAS software, (http://currents.soest.hawaii.edu/docs/adcp_doc/codas_setup/index.html) following the procedure of Hummon and Firing (2003). Data presented are averages over the top 150 m.

2.1.2 **Temperature and salinity**

An on-board thermosalinograph continuously measured sea surface temperature (SST) and salinity (SSS). At each station, Conductivity Temperature Depth (CTD) casts down to 500 m recorded continuous vertical profiles of temperature and salinity. CTD data were checked for spurious values using the Seasoft software (Sea-Bird electronics, Washington, USA), binned at 1m intervals and presented for the top 200 m.

2.1.3 **Water sampling**

Water was sampled during the CTD casts using 8 L Niskin bottles to measure nutrients, chlorophyll, phytoplankton cell counts, photosynthetic pigments and primary production. Depth and frequency of sampling varied according to variables measured and associated analyses (Table 1).

2.1.4 **Nutrients**

Nitrate, phosphate (Soluble Reactive Phosphorus: SRP) levels were measured in $HgCl_2$-poisoned samples and analyzed in the laboratory within two months of the end of the cruises using an Auto-analyzer AA3 (Bran+Luebbe, Norderstedt, Germany), as described in Aminot and Kérouel (2007). Nitrate and nitrite (reported as NO_3) concentrations were determined at nanomolar precision (Raimbault et al., 1990). SRP concentrations (reported

Accepted manuscript

as PO_4) were analyzed according to Murphy and Riley (1962). Data were interpolated to plot the 0-180 m vertical profiles using Dr Masson's SAXO package (http://forge.ipsl.jussieu.fr/saxo/download/xmldoc/whatissaxo.html) based on IDL (Interactive Data Langage, Exelisvis, Boulder, USA).

2.1.5 **Phytoplankton: biomass and community structure**

Phytoplankton composition and community structure were identified from water samples collected (Table 1) and results were averaged across the depths: 0-50 m and 50-130 m.

2.1.5.1 Chlorophyll

In situ chlorophyll a (Chl-a) values were determined after methanol extraction (Le Bouteiller et al., 1992), using a Turner Design fluorometer (Turner Designs, Sunnyvale, California, USA, module # 7200-040, Chl-a extracted-acidification) calibrated with pure Chl-a standard (Sigma). Total Chl-a concentrations were determined from 0.5 L water samples filtered onto GF/F Whatman filters. Size-fractioned Chl-a across the size classes <3 µm, 3-10 µm and >10 µm was determined from 2 L water samples collected onto 10 µm, 3 µm nucleopore and GF/F filters by in-line serial filtrations, and represented proxies of pico-, nano and microphytoplankton biomasses respectively. The mean and standard deviation of size-fractionated Chl-a percentages were calculated for each cruise. Total Chl-a data were interpolated to plot the 0-150 m vertical sections of each cruise using the SAXO package.

2.1.5.2 *Cell counts by flow cytometry (FCM)*

Water samples of 1.1 mL were fixed by adding paraformaldehyde solution (2% final concentration) and then frozen in liquid nitrogen on board. Cell counts for pico and nanophytoplankton (<3 µm, 3-10 µm respectively) were performed with a FACSCalibur flow cytometer (BD Biosciences, San Jose, California, USA) at the Regional Flow Cytometry Platform for Microbiology (PRECYM) (http://precym.com.univ-mrs.fr). Data were normalized using both Fluoresbrite® Fluorescent Microspheres (Polysciences Inc. Europe) and TruCountTM beads (BD) and the mean and standard deviation of cell count percentages were calculated for each cruise.

Accepted manuscript

2.1.5.3 Phycoerythrin

Water samples (4.5 L) were filtered onto 0.4 µm Nucleopore polycarbonate membrane filters (47 mm diameter) and immediately frozen in liquid nitrogen until analysis. Using methods described in Neveux et al. (2009), phycoerythrin (PE) was extracted in a 4 mL glycerol-phosphate mixture (50/50) after vigorous shaking for resuspension of particles (Wyman, 1992). Using a Perkin Elmer LS55 spectrofluorometer (PerkinElmer, Inc., Waltham, Massachusetts, USA) and emission and excitation slit widths adjusted to 5 and 10 nm, respectively, the PE fluorescence excitation spectra were recorded between 450 and 580 nm (emission fixed at 605 nm). Quantitative estimates of phycoerythrin were obtained from the area below the fluorescence excitation curve, after filter blank subtraction and the mean and standard deviation calculated for each cruise.

2.1.6 **Primary production**

Net primary production (NPP, mgC m^{-3} d^{-1}, Table 1) was measured using the ^{14}C tracer technique (RochelleNewall et al., 2008). Water samples (76 mL) were inoculated with 0.40 MBq of a sodium ^{14}C bicarbonate solution (Perkin Elmer, initial concentration 37 MBq mL^{-1}) and immediately placed in a thermoregulated (22-24°C) photosynthetron to incubate samples at varying light levels (11%, 28%, 48%, 68%, 100%). After 1.5 h incubation, samples were filtered onto 0.4 µm polycarbonate filters (25 mm Whatman Cyclopore) which were then placed into clean glass liquid scintillation counting vials and stored at -20 °C. In the laboratory, 100 µL of 0.5N HCl was added to each sample, and the vial left open for 12 h under a fume hood to remove unfixed ^{14}C. After acidification and drying, 5 mL of scintillation cocktail (Ultima Gold MV, Parkard instruments) was added to each sample, and the samples analyzed in a Packard Tri-Carb (1600TR) Liquid Scintillation Counter (PerkinElmer, Inc., Waltham, Massachusetts, USA). The mean and standard deviation were calculated for each cruise.

2.1.7 **Zooplankton**

Three methods were used to estimate zooplankton (organisms 2 µm – 20 mm) biomass: a Tracor Acoustic Profiling System (TAPS), net sampling and Ship-Borne Acoustic Doppler Current Profilers (S-ADCP).

Accepted manuscript

ACCEPTED MANUSCRIPT

2.1.7.1 Tracor Acoustic Profiling System (TAPS)

The TAPS-6™ (BAE systems, San Diego, CA, USA) is a six frequency (265, 420, 710, 1100, 1850, 3000 kHz) profiler (Holliday and Pieper, 1980) used to acoustically detect the micro- (20-200 µm) and meso- (200-2000 µm) zooplankton from the surface down to 200 m. The TAPS-6 was used in "cast mode", profiling the water column in horizontal position with a descent speed of 0.5 m s^{-1}, sampling a volume of about 5 L of water at each ping (ping rate: 2.63 pings s^{-1}). The TAPS-6 focused on small and abundant organisms such as copepods, with larger and less abundant organisms such as euphausiids having less chance to pass through this small volume (Pieper et al., 2001).

The Scattering Volume (Sv) signal (in dB) was transformed into biovolume estimates using an inversion algorithm following the method applied by Lebourges-Dhaussy et al. (2014) and successfully applied to small zooplankton (e.g. Holliday et al., 1989; Lebourges-Dhaussy et al., 2009; Napp et al., 1993; Pieper et al., 1990). The algorithm provided vectors of abundances per size range for each station, from which biovolumes were estimated in mm^3 m^{-3} and converted into mg m^{-3} using a density factor of ~1 kg L^{-1} (Simmonds and MacLennan, 2005). The size range of organisms explored in the inversion process was 0.05-3 mm (micro- and meso-zooplankton).

2.1.7.2 Zooplankton net sampling

Five layers of the water column were sampled from the surface down to 600 m depth (0-100, 100-200, 200-400, 400-500, 500-600 m) using an Hydrobios MultiNet (Hydrobios, Kiel, Germany). Each of the nets used were comprised of 200 µm nylon mesh and equipped with a mechanical Hydrobios flowmeter. The volume filtered by each net was calculated using the following equation:

$$V=d*k*A$$

where d is the number of revolutions of the flowmeter, k=0.3 m/revolution is the pitch of the impeller of the flowmeter provided by the manufacturer (Hydro-Bios Apparatebau GmbH, 2009) and A is the size of the net mouth area (0.25 m^2).

Accepted manuscript

ACCEPTED MANUSCRIPT

Samples collected by the nets were immediately preserved in a 5 % buffered formalin-seawater solution and processed for wet and dry weight analysis later in the laboratory. Dry weights (DW) and wet weights (WW) were determined for the 0-200 m and the 0-600 m layers respectively.

2.1.7.3 Ship-Borne Acoustic Doppler Current Profilers (S-ADCP) backscatter

The S-ADCP (see section 2.1.1), was also used to provide relative measures of acoustic density, as a proxy for zooplankton to micronekton biomass (Flagg and Smith, 1989; Heywood et al., 1991; Menkes et al., 2002; Radenac et al., 2010). At 153 kHz, this instrument roughly detects organisms across the size ranges of a few millimeters to a few centimeters (Sutor et al., 2005). The ADCP echo intensity (E_a) was converted into S_v (in dB) using the equation from Deines (1999) modified by Gostiaux and van Haren (2010):

$$Sv=C+10\log_{10}[(T_x+273.16)R^2]-L_{DBM}-P_{DBW}+2\alpha R+10\log_{10}[10^{KcEa/10}-10^{KcEnoise/10}]$$

where T_x is the temperature of the transducer (°C), L_{DBM} is $10\log_{10}$(transmit pulse, in meters), P_{DBW} is $10\log_{10}$(transmit power, in Watts), R is depth along the beam (m), α is the sound absorption coefficient (dB/m) in water, K_c is a conversion factor for echo intensity (dB/counts), E_a is the ADCP raw echo intensity (counts) and E_{noise} is the noise (counts). We used the default parameters given in Deines (1999) for the constants C and P_{DBW}. During the time that the ship was stationary at each station, when ship noise is reduced, we selected the minimum value of the echo intensities E_a in the vertical profiles and the minima were then averaged over the entire cruise to obtain E_{noise}.

2.1.8 **Micronekton**

Three methods were used to estimate micronekton (organisms 2 - 20 cm) biomass and species composition: using an EK60 echosounder, net sampling and the S-ADCP (see section 2.1.7.3).

2.1.8.1 EK 60 echosounder

Acoustic data were collected continuously during the cruise using a EK60 echosounder (SIMRAD Kongsberg Maritime AS, Horten, Norway) with four hull-mounted split-beam transducers (38, 70, 120 and 200 kHz). Echosounder calibration was performed according to

Accepted manuscript

ACCEPTED MANUSCRIPT

Foote et al. (1987) at the beginning of each cruise. Due to the presence of noise in echograms, linked to the specificities of the installation of the sounder on the R/V Alis and to rough seas during the cruises, the water column was only sampled down to depths of 100, 200, 250 and 600 m for the 200, 120, 70 and 38 kHz channels respectively. A data cleaning step was performed with Matlab® (MathWorks, Natick, Massachusetts, USA) filtering tools provided with the Movies3D software (IFREMER). The EK60 signal was analyzed in terms of scattering volume (Sv) (MacLennan et al., 2002). It was not possible to calculate micronekton biomass from echograms produced as the Sv to biomass conversion requires knowledge of the acoustic properties of the detected organisms added to a complex inversion of the signal and has not yet been performed for our dataset. The 38 kHz frequency is commonly used as a proxy for micronekton (Bertrand et al., 1999; Kloser et al., 2009; McClatchie and Dunford, 2003) and was used to represent micronekton over 0-600 m.

To describe the spatial structure of the micronekton biomass derived from the 38 kHz EK60, we removed the day/night signal from the data as the strong diurnal vertical migration of micronekton might mask spatial patterns. The data were assigned to either day or night and average values were calculated for each period for each cruise. The daytime (resp. nighttime) mean was subtracted from the daytime (resp. nighttime) values to produce anomalies for each period.

2.1.8.2 Micronekton net sampling

Micronekton were sampled at each station with a mid-water trawl with a 10 mm codend mesh size. Vertical and horizontal mouth opening of ~10 m each were monitored with trawl opening sensors (Scanmar, Åsgårdstrand, Norway). Horizontal tows were conducted to target aggregations visually detected with the EK60 echosounder. Once the trawl net was stabilised at the chosen depth, it was towed for 30 minutes at 3-4 knots. One or two tows were conducted at each sampling station between 14 and 130 m at night and between 21 and 540 m during the day. Organisms were sorted on-board into groups and frozen. In the laboratory, samples were identified at the lowest taxonomic level possible, counted, measured and weighed. Gelatinous organisms (e.g. siphonophores, salps, pyrosomes) were

Accepted manuscript

weighed frozen as a group. Biomass was expressed as mg of wet weight per m^3 filtered. The volume of water filtered by the net was calculated as:

$V=S*D$,

with $S=h*v$ and $D= R*c$,

$$c = 2*\arctan(\sqrt{a/(1-a)})$$

and $a=[\sin((lat_2-lat_1)/2)]^2 + \cos(lat_1)*\cos(lat_2)*[\sin((lon_2-lon_1)/2)]^2$

where V is the volume filtered (m^3), S is the net mouth opening (m^2), h and v are the net horizontal and vertical mouth opening (m), D is the distance covered by the trawl (m), $R=6371.e^{+3}$ m is the earth radius, lat_1, lat_2, lon_1, lon_2 are the latitude and longitude of the start and the end of the set (radian).

2.2 Other in situ, satellite and model derived datasets

Estimated oceanographic and biological parameters derived from remote sensing and physical and biological models were used to undertake direct comparisons between *in situ* data and satellite and model derived parameter estimates and investigate relationships of in situ data collected during each cruise with broader scale regional ocean dynamics .

2.2.1 **Ocean Currents**

We used two datasets, the Kessler and Cravatte (2013) *in situ* dataset and the Ocean Surface Current Analysis (OSCAR, http://www.oscar.noaa.gov/) satellite-derived dataset. The first describes the time-averaged total geostrophic circulation of the top 1000 m. The second provides surface currents estimated from a combination of data derived from drifting buoys and altimetry at a 5-day and 1/3^o resolution.

2.2.2 **Eddies: Okubo-Weiß parameter**

Surface ocean dynamics were examined using an eddy detection algorithm. The Okubo-Weiß (OKW) parameter was calculated from the OSCAR surface currents. It describes the

Accepted manuscript

ACCEPTED MANUSCRIPT

deformation (shear and strain) and rotation (vorticity) of surface currents (Chelton et al., 2011b; d' Ovidio et al., 2013; Dutrieux et al., 2008). This parameter allows discrimination of regions where fluids circulate in a closed loop (OKW < 0, e.g. in the interior of eddies where vorticity is high) from regions where shear and strain are high (OKW > 0, e.g. on the edges of eddies where strain is high). The OKW parameter is always negative within vortices whether they are cyclonic or anticyclonic (Chelton et al., 2011b).

2.2.3 **Sea Level Anomaly (SLA)**

Sea level anomalies (relative to the long term mean across the period 1993-2010) were extracted from http://www.aviso.oceanobs.com/en/data/products/sea-surface-height-products/global/msla.html#c5122 at a resolution of 1/3° and 7 days. SLA was used to identify downwelling (high values or ridges in SLA) versus upwelling eddies (low values or troughs in SLA).

2.2.4 **Sea Surface Temperature (SST)**

Daily SSTs from the Group for High Resolution SST (GHRSST) were downloaded from the website https://www.ghrsst.org/ and used to examine spatial patterns in SSTs in the New Caledonian EEZ. This freely available product combines several satellite data sources and is provided at 1/12° grid resolution.

2.2.5 **Primary production**

Depth-integrated primary production was estimated from satellite-derived chlorophyll, Photosynthetically Available Radiation (PAR) fields and SST fields using the Vertically Generalized Production Model (VGPM) (Behrenfeld and Falkowski, 1997). Primary production was integrated across the euphotic layer, which was statistically derived from satellite imagery (http://www.science.oregonstate.edu/ocean.productivity/). Satellite-derived chlorophyll is calculated from ocean color data, which, for the period 2002-2009, were derived from the Sea-viewing Wide Field Of View Sensor (SeaWiFS) satellite after which data were computed at CLS (www.cls.fr) using the VGPM model and Moderate Resolution Imaging Spectroradiometer (MODIS) and Medium Resolution Imaging Spectrometer (MERIS) satellite data. PAR data were derived from the European Center for Medium Range Forecast (ECMWF) analyses.

Accepted manuscript

ACCEPTED MANUSCRIPT

2.2.6 Micronekton from the SEAPODYM model

The end-to end spatial ecosystem model SEAPODYM (Lehodey et al., 2008) describes the interactions of tuna species with the environment and incorporates external forcings associated with fishing and the environment. It includes environmental parameters such as temperature, currents, oxygen and primary production as well as a micronekton sub-model describing the transfer of energy from primary production to tuna species through mid-trophic levels. The sub-model comprises six functional groups of micronekton occupying different water layers according to day and night (diel migration model). Modelled micronekton is advected by currents and assimilates carbon from primary production produced three months earlier (Lehodey et al., 2010).

The micronekton sub-model is driven by satellite-derived primary production (see section 2.2.5) and by the outputs of the GLobal Ocean ReanalYsis and Simulations (GLORYS2.V1) of currents and temperature produced by the French Groupe Mission Mercator Coriolis (Barnier et al., 2006; Ferry et al., 2012) across two reanalysis periods 2002 – 2008 and 2009 - 2012. The 2002 – 2008 reanalysis was conducted at a daily and 1/4° resolution and was performed by the MERCATOR-OCEAN operational oceanography center. It is forced by daily surface meteorological data from the European Centre for Medium-Range Weather Forecasts (ECMWF). By assimilating satellite-derived sea level anomalies, sea surface temperatures and *in situ* measurements of vertical temperature and salinity profiles, the model estimates realistic mesoscale activity with eddy field variability in good agreement with altimetric data. Reanalysis across 2009-2012 included temperature and currents provided by the same numerical ocean model, while altimetry, SST and temperature/salinity profiles were also assimilated in their operational configuration (http://www.mercator-ocean.fr/)(Abecassis et al., 2013).

The biomass distribution of micronekton functional groups along the cruise track and in the south-west Pacific at the time of the cruises was estimated with the SEAPODYM ecosystem model using a revised definition of vertical biological layer boundaries, at a spatial resolution of 1/4° averaged over 7 days. Vertical biological layers comprised the epipelagic layer, which lies between the surface and the euphotic depth (derived from ocean color

Accepted manuscript

satellite data and the VGPM model), the mesopelagic layer located at 1-3 times the euphotic depth, and the bathypelagic layer located at 3-7 times the euphotic depth. The model simulates a diel behavior of micronekton by considering that during the night, daily migratory species can move from one layer to another, thus adding to the residing biomass of non-migratory species of the layer. Because we used 7-day outputs to compare with the continuous Nectalis data, we reconstructed a SEAPODYM time series with a day/night signal that mimicked the Nectalis data. We interpolated the Nectalis tracks into the SEAPODYM model. This interpolation was temporally referenced so that day and night estimates from SEAPODYM could be extracted.

To describe the spatial structure of the micronekton biomass derived from SEAPODYM, we removed the day/night signal from the data by calculating anomalies following the same procedure than for 38 kHz EK60 (see section 2.1.8.1).

2.3 Statistics and comparison of methods

2.3.1 **Primary production**

The non-parametric rank-sum Wilcoxon-Mann-Whitney test at α=5% was used to test the seasonal difference in *in situ* primary production values and in VGPM satellite-derived primary production along the cruise track. Spatial auto-correlation was eliminated from the VGPM dataset by building a new dataset of independent points before conducting the seasonal comparison.

To build this new dataset of independent points, we determined the distance (“d” in km) at which two points are independent. The initial auto-correlated dataset was then resampled selecting a point every “d” kilometers creating a dataset of independent points. Shifting the start position of this subsampling by 1 km, another dataset of independent points was then created. This procedure was repeated until the number of resampled datasets of independent points was equal to “d”, and contained a number “n” of independent points which was the length of the cruise track divided by “d”. In the statistical tests the “d” resampled datasets of independent points were all tested and the result of the test

Accepted manuscript

ACCEPTED MANUSCRIPT

(difference or no difference) comes with the percentage of the number of "d" tests producing this result.

To estimate the distance "d" between two independent points, empirical spatial variograms with 10km bins were used. The variogram of the VGPM dataset was compared to the noise constructed from a series of variograms of 100 randomly re-ordered VGPM datasets by a Monte Carlo procedure. The distance "d" at which the dataset points become uncorrelated was estimated when the variogram of the dataset reached the noise.

For the VGPM dataset "d" was estimated at ~50 km during Nectalis1 and 100 km during Nectalis2. Overall a conservative value of 100 km between two successive data points was considered, prompting ~ 100 possible VGPM datasets of 30 independent points (or, equivalently degrees of freedom) for Nectalis1 and 35 independent points for Nectalis2. These 100-ensemble datasets were used for seasonal comparisons.

We estimated that *in situ* primary production points were independent (no spatial auto-correlation) on the basis that the minimum distance between two sampling stations where *in situ* primary production was measured (144 km) is greater than the estimate at which 2 points were determined to be independent using the VGPM dataset (100 km).

The Wilcoxon-Mann-Whitney test at α=5% was also used to compare *in situ* primary production to VGPM data at the location of the *in situ* measures (12 data points). For small sample sizes, values for significance were read in classical tables, while where sample sizes were n>20 degree of freedom, the test was calculated using IDL's routines (imsl_wilcoxon.pro).

2.3.2 **Zooplankton**

A Wilcoxon-Mann-Whitney test at α=5% was used to test for seasonal difference in zooplankton biomasses estimated from the zooplankton net (in DW and WW), the TAPS and the S-ADCP backscatter. We accounted for the spatial auto-correlation of the S-ADCP by following the procedure described in section 2.3.1. For the S-ADCP dataset, the distance "d" at which two points were considered independent was 30 km for both cruises. Consequently, 30 datasets of 100 and 116 independent points were built for Nectalis1 and

Accepted manuscript

ACCEPTED MANUSCRIPT

Nectalis2 respectively for statistical analyses. We estimated that *in situ* zooplankton biomass estimates (zooplankton net and TAPS) points were independent (no spatial auto-correlation) on the basis that the minimum distance between two sampling stations (67 km) is greater than ”d” (30 km).

The potential for the S-ADCP to provide a proxy of zooplankton biomass was evaluated against the log-transformed biomass measurements of zooplankton derived from the TAPS and net sampling using a Spearman’s correlation.

For this general overview, no detailed examination of zooplankton spatial distribution and composition were conducted, but will be conducted in a separate study (Smeti pers. comm.).

2.3.3 **Micronekton**

A Wilcoxon-Mann-Whitney test at α=5% was used to test for seasonal differences in micronekton biomass estimated by the EK60 and by the SEAPODYM ecosystem model. No seasonal comparison was conducted on net sampling because of differences in sampling strategies between the two cruises (non-comparable depth or day-night tows). We accounted for the spatial auto-correlation of the 38 kHz EK60 Sv and SEAPODYM micronekton biomass estimates by following the procedure described in section 2.3.1. For the 38 kHz EK60 Sv dataset the distance “d” at which two points were considered independent was 30 km for both cruises. Consequently, 30 datasets of 100 and 116 independent points were built for Nectalis1 and Nectalis2 respectively for statistical analyses. For the SEAPODYM dataset, “d” was estimated at 100 km for Nectalis1 and 50 km for Nectalis2. A conservative value of “d”=100 km was used for both cruises to build 100 datasets of 30 and 35 independent points for Nectalis1 and Nectalis2 respectively.

The potential for the S-ADCP to provide a proxy of micronekton biomass was evaluated against the Sv values of the four frequencies of the EK60 echosounder. To do this, the EK60 high-resolution time and vertical profiles were averaged to the ADCP time/vertical resolution. The Sv was calculated for a 5-minute Elementary Sampling Unit (ESU) and 8 m height layers. Correlations between data provided by the S-ADCP and the four frequencies

Accepted manuscript

of the EK60 were investigated using a Spearman's correlation. We accounted for the spatial auto-correlation by computing 30 correlation coefficients from the 30 resampled datasets of independent points distant of 30 km, as explained above. The range of correlation coefficients from the 30 correlation ensemble was provided as well as the percentage of these correlations significant at α=5% level.

Estimates of epi and mesopelagic micronekton biomass (mg m^{-3}) derived from SEAPODYM were compared to the estimates of micronekton biomass derived from the 38 kHz EK60 echosounder. The high-resolution EK60 data were averaged across ¼ degree grid squares along the cruise track to correspond with the spatial resolution of the SEAPODYM ecosystem model. Correlation between the two data series was investigated applying the same procedure as for EK60 *vs.* S-ADCP. and accounting for the Spatial auto-correlation was accounted for by calculating the correlation on 100 resampled datasets of independent points distant of 100 km from the two biomass series..

3 Results

3.1 Physical oceanography and biogeochemistry

3.1.1 **Surface features**

During the cool season (Nectalis1) thermosalinograph measurements showed that surface waters in the southern part of the cruise track (south of 19°S) had an average temperature of 23.6 ± 1.0 °C and salinity of 35.2 ± 0.2 while the northern part of the cruise was characterized by waters of 25.3 ± 0.7°C and 35.0 ± 0.1 (Figure 2). During the hot season (Nectalis2), overall SST and SSS patterns were similar, although temperatures were warmer by ~3°C. Salinity was very similar in the south but lower by ~0.1 in the north (Figure 3). During both cruises, salinity varied across similar gradients to temperature, but in the opposite direction at both larger-scales and smaller scales. For example, high temperature and low salinity waters were observed during Nectalis1 at stations 4 and 5 with waters with

Accepted manuscript

ACCEPTED MANUSCRIPT

particularly low temperature and high salinity observed at stations 1 and 2 during both cruises. This gradient was observed in particular during Nectalis2.

During both cruises, ADCP surface layer (0-150 m) currents varied in a similar way across large and small spatial scales to surface-only currents derived from OSCAR. North of 19°S, the currents were predominantly directed westward, while in the south they were predominantly directed eastward. Along the western coast of the main island of New Caledonia, currents were flowing predominantly south-eastward during Nectalis1 and southward during Nectalis2. In addition to these broad scale patterns, high current variability was observed, for example at stations 6-7 during Nectalis1 and stations 7-8-9 during Nectalis2.

Satellite-derived SST clearly showed the large-scale north-south gradient in observed during both cruises. Smaller scale meandering of the SST field centered at ~19-20°S was observed with strong association between the thermohaline patterns and the currents. Meanders were noted through intrusions of warmer waters from the north which were advected south (e.g. Nectalis1 station 8, 17, Nectalis2 station 9) and intrusions of cooler waters from the south which were advected north (e.g. Nectalis1 stations 6, 7, 16, Nectalis2 stations 17-18).

Values of OKW and SLAs along with current vectors from both OSCAR and S-ADCP described an important turbulent eddy activity. Cyclonic eddies ("upwelling" type eddy) corresponding to sea level depression (or equivalently, thermocline uplifting) were observed during the cool season, for example at ~23°S 161°E (eddy A on Figure 2), at stations 6-7 (eddy B) and at ~16.5°S 159°E (eddy C) the south-eastern edge of which was sampled at station 10 (Figure 2). During the hot season, strong cyclonic eddies were observed at ~24°S 156°E (eddy D on Figure 3), ~24°S 164°E (eddy E) and ~25°S 172°E (eddy G) and a series of energetic eddies were observed between stations 7 and 18 (eddies H, I, J). The edge and the center of an anticyclonic eddy ("downwelling" type eddy with thermocline deepening and sea-level ridge) were sampled during the hot season at stations 8 and 9 respectively (eddy K, Figure 3). Overall, lower eddy activity was observed during the cool season (Figure 2) than during the hot season (Figure 3).

Accepted manuscript

3.1.2 **Vertical structures**

During the cool season, stations 8 - 18 in the north and east were characterized by relatively warm, low salinity waters with a mixed layer depth of ~60m and low values of nitrate (0.05 ± 0.07 µM) to a depth of ~90 m (Figure 4). The Deep Chlorophyll Maxima (DCM) (~0.25-0.3 mg m^{-3}) and the nutricline were located at ~90 m depth (Figure 4). By contrast, stations 1 - 7 in the south and west were comparatively cooler with higher surface salinity. At these stations, higher concentrations of nitrate (0.13 ± 0.12 µM) and chlorophyll content occurred with more frequent maxima at the surface. Phosphate concentrations varied with an average of 0.067 ± 0.038 µM from the surface to 100 m depth and were occasionally lower than 0.05 µM in the surface layer. Within this general pattern, a number of stations demonstrated unique characteristics. Cool, highly saline waters which were homogeneous down to 100 m with a shallow nutricline and enhanced chlorophyll were recorded at stations 1 and 2 (Figure 4). Waters with a deep mixed layer, elevated chlorophyll from the surface down to 100 m were also recorded at stations 6 and 7, contrasting with the surrounding waters (Figure 4). High surface (0-20 m) chlorophyll levels (0.23 µg l^{-1}) were recorded at station 10 (Figure 4).

The north-south gradient in temperature and salinity observed during the cool season was also evident at depth during the hot season, with warmer and fresher waters north of ~20°S observed at stations 8 - 19 (Figures 3 and 4) and cooler and saltier waters south of ~20°S observed at stations 1 - 7 and 20 to 23 . The mixed layer across all stations was shallower during the hot season, located at ~25 m, denoting stronger surface stratification in the water column than during the cool season. Surface waters were low in nitrate (0.03 ± 0.02 µM) across almost the entire cruise track (Figure 4) and the DCM was often centered at around 100 m with mean values of ~0.41 ± 0.16 mg m^{-3}. In general, above the DCM in the top ~ 50 m, chlorophyll concentrations were slightly lower than during the cool season (Figure 4), particularly in the southern part of the survey area. Phosphate tended to be low (0.05 ± 0.03 µM) for stations 1 - 7 and 20 - 23 in the southern part of the cruise track in comparison to stations in the northern part of the cruise (0.09 ± 0.03 µM). A few stations had unusual characteristics: high temperatures and low salinities down to 100 m were

Accepted manuscript

ACCEPTED MANUSCRIPT

observed at station 9 and surface nitrate was slightly enhanced at stations 7 and 8 (0.09 ± 0.01 µM) compared to other stations (0.02 ± 0.02 µM).

3.2 Primary production

Depth- integrated measurements of *in situ* primary production in the photic layer and similar satellite-derived net primary production (NPP) from VGPM along the cruise track were significantly higher during the cool season (352±160 mgC m^{-2} d^{-1} and 301±62 mgC m^{-2} d^{-1} on average respectively) than during the hot season (231±133 mgC m^{-2} d^{-1} and 199±55 mgC m^{-2} d^{-1}) (Figure 5 and Table 2)

The NPP pattern (Figure 2) demonstrated a strong gradient during the cool season with values of ~350 mgC m^{-2} d^{-1} in the southern part of the survey area (south of 20°S and west of the main island) and values lower than 200 mgC m^{-2} d^{-1} in the northern part of the survey area (north of 20°S and east of the main island). During the hot season the entire region was more oligotrophic, with a weaker north-south gradient, and average values of ~200 mgC m^{-2} d^{-1} in the survey area (Figure 3). Within this large-scale gradient, specific patterns linked to mesoscale structures were observed. For example, the center of some eddies were characterized by enhanced primary production (e.g. Nectalis1 eddy A; Nectalis2 eddy D; Nectalis2 eddy G), while primary production was enhanced at the edge of others (e.g. Nectalis1 station10 eddy C; Nectalis2 series of eddies H, I, J).

No significant differences were found between *in situ* production estimates and VGPM satellite values at the *in situ* sample locations (Figure 5).

3.3 Phytoplankton

During the cool season, size fractionated chlorophyll was dominated by picophytoplankton (< 3 µm) across all stations (mean=75.9% ± SD=17.2% in biomass); nano and micro-phytoplankton represented 12.8% ± 9.6% and 11.3% ± 12.6% respectively of chlorophyll biomass. The cyanobacteria *Prochlorococcus* were the dominant species of the

Accepted manuscript

ACCEPTED MANUSCRIPT

picophytoplankton group (91.9% ± 6.3% in abundance; Figure 4) with cell abundances of up to 250 x 10^3 mL^{-1}. Remaining abundances of picophytoplankton across stations were comprised of *Synechococcus* (6.3% ± 6.2%) and picoeukaryotes (1.8% ± 0.8%). Overall phytoplankton composition did not vary latitudinally or longitudinally, with the exception of particular features observed at stations 2 and 10 (eddy C). In comparison to other stations, higher proportions of large cells were observed at station 2 from the surface to 150 m (~30% nano- and ~28% microphytoplankton in abundance) and at station 10 from the surface to 50 m (~17% nano- and ~31% microphytoplankton in abundance).

The fractionated chlorophyll and community structure during the hot season was similar to that observed in the cool season with picophytoplankton and *Prochlorococcus* dominating the communities (83.4% ± 10.4% in biomass and 92.3% ± 7.8% in abundance respectively; Figure 4). Nano and micro-phytoplankton represented 8.6% ± 5.4% and 7.9% ± 7.1% respectively. However, cell abundance was much lower during the hot season, with maximum cell counts of *Prochlorococcus* of 160 x 10^3 mL^{-1}. Remaining cell abundances were comprised of *Synechococcus* (5.0% ± 6.8%) and picoeukaryotes (2.7% ± 1.7%). Again, the phytoplankton structure was relatively homogeneous along the cruise track with the exception of station 9 (eddy K) which had a higher proportion of larger cells from the surface to 50 m (~7% nano- and ~39% microphytoplankton in abundance) than the rest of the stations (~13% ± 3.1% nano- and ~11%±5.0% microphytoplankton in abundance; Figure 4). Phycoerythrin (PE) concentration was also much higher at this station (1836 fluorescence unit *vs.* 389 ± 359 fluorescence unit for the other stations).

3.4 Zooplankton

Diurnal variability in zooplankton biomass was observed with all methods, with enhanced biomass at night in the top 200 m during both cruises (Figure 6 and 7). Zooplankton WWs during the hot season however were relatively similar during the day and at night, which is at odds with dry weight (DW) estimates where diurnal variability is evident (Figure 6 and 7). Zooplankton wet weight (WW) (Figure 6) vertical profiles showed that the majority of the biomass concentrated in the top 100 m, deeper biomass rapidly decreased.

Accepted manuscript

ACCEPTED MANUSCRIPT

Mean biomass estimates from the TAPS (~ 100 mg m^{-3}) were more than one order of magnitude higher than WW estimates from net samples (< 6.5 mg m^{-3}) and DW estimates from net samples (< 6 mg m^{-3}) (Table 2). Zooplankton biomasses derived from TAPS and WW estimates across all sampling stations were not significantly different between the two cruises, while significant differences were observed in DW (Nectalis1<Nectalis2) and S-ADCP (Nectalis1>Nectalis2) estimates (Table 2).

Correlations between acoustic biomass proxies and net biomass measures for zooplankton were all significant, with the TAPS and S-ADCP having the highest correlation overall (Table 3). Estimates derived from net samples demonstrated similar correlations with those derived from the S-ADCP and those derived from the TAPS (Table 3). Correlation values between zooplankton measurements were roughly similar across the two depth ranges explored: 0-100 m and 0-200 m.

3.5 Micronekton

Preliminary examination of the micronekton composition indicated that micronekton net catch was dominated by gelatinous organisms (e.g. siphonophores, salps, pyrosomes), which represented 53.8% of the overall wet weight biomass. Fish, molluscs and crustaceans represented 36.5%, 7.6% and 2.1% of the biomass, respectively. In total, approximately 480 taxa were identified, including ~240 fish taxa, ~95 crustacean taxa, ~85 mollusc taxa and ~60 gelatinous organism taxa. Of those species able to be identified, those species with the highest biomasses in each taxa group were the lanternfish *Ceratoscopelus warmingii*, *Hygophum hygomii* and *Diaphus perspicillatus*; the molluscs *Sthenoteuthis oualaniensis, Abraliopsis sp.* and *Abralia omiae*; and the crustaceans *Thysanopoda tricuspidata, Thysanopoda cristata* and *Euphausia mucronata*. Of the gelatinous organisms the most abundant were Pyrosomatidae, Abylidae and *Pyrosoma atlanticum*.

Biomass estimates from *in situ* measurements from the micronekton nets for the 0-600 m and from SEAPODYM model were in the same range: ~ 4 mg m^{-3} (Table 2).

Accepted manuscript

During both seasons, the EK60 and SEAPODYM signal anomalies indicated that the region north of ~19°S-20°S had lower micronekton biomass than the region south of this latitude (Figure 8). Smaller scale variability was also apparent in both datasets, most prominently south of 19°S-20°S where patches of higher biomass were observed; for example along the west coast of the main island and at ~20.5°S 161°E during Nectalis1 and ~20.5°S 158°E during Nectalis2.

Micronekton abundance estimated from the S-ADCP, the nets, the EK60 and the SEAPODYM model exhibited a clear maximum at night (Figure 7). Vertical profiles of the micronekton estimated from the 38 kHz EK60 Sv (Figure 6) demonstrated a bimodal distribution with higher micronekton biomass estimates occurring at 0-200 m and 400-600 m than at other depths during both the day and night.

Seasonal differences observed in micronekton biomass estimated by the EK60 Sv and SEAPODYM were not statistically significant (Table 2). Conversely, estimates derived from the S-ADCP were different with higher values during the cool season (Table 2).

Micronekton estimates derived from the EK60 Sv and S-ADCP Sv were highly correlated, and the highest correlation was observed with the 70 kHz EK60 (correlation range = 0.87-0.96) (Table 4). Micronekton biomass estimates calculated by the 38 kHz EK60 Sv were highly correlated with estimates derived from the SEAPODYM model (correlation range = 0.73-0.79) (Table 4).

4 Discussion

4.1 Oligotrophic waters and water masses

The physical, biogeochemical and biological data collected during the two Nectalis cruises, in two contrasting seasons, have provided new insights into the spatial and temporal dynamics of the pelagic ecosystem in the waters around New Caledonia. Observations collected from the two cruises support prior characterization of the region as oligotrophic. The vertical nutrient profiles, low nitrate and sometimes low phosphate, low primary

Accepted manuscript

ACCEPTED MANUSCRIPT

production and chlorophyll biomass, and a phytoplankton composition dominated by small size cells (picophytoplankton), were consistent with previous studies in South Pacific region (Campbell et al., 2005; Jacquet et al., 2006; Young et al., 2011) and are typical of a Low Nutrient Low Chlorophyll (LNLC) system. Although it is generally thought that nitrate is the main limiting nutrient in this oligotrophic region (Le Borgne et al., 2011), some phytoplankton species may be limited by phosphate (Moutin et al., 2005) and this can induce higher contributions of diazotrophs such as *Trichodesmium sp.* in this area. *Trichodesmium sp.* was not observed in the samples we collected, but it was seen at the surface of the water along the track at one occasion. Examination of isotope values calculated from biological samples collected during the Nectalis cruises (Hunt et al., this issue) suggests the contribution of diazotrophs to phytoplankton composition as previously observed in the area (Campbell et al., 2005; Dupouy et al., 2011).

Two distinct water masses were encountered in the studied area. North of 19°S-20°S, waters in the top 200 m were characterized by warm temperature, low salinity, low nitrate, lower primary production and lower micronekton biomass estimates. These characteristics are representative of the “Coral Sea” oligotrophic regime (Ceccarelli et al., 2013), and are largely influenced by the warmer and fresher waters of the south Pacific convergence zone (SPCZ) where the SEC predominantly flows,.

South of 19°S-20°S, waters are characterized by colder temperature, higher salinity, a shallower nitracline, higher nitrate content in the surface layer, higher primary production and higher micronekton biomass estimates and are under the influence of the South Tropical Counter Current branches (Marchesiello et al., 2010).

Although water masses were variable latitudinally, phytoplankton compositions were very similar throughout the whole area.

4.2 Horizontal advection, mesoscale and submesoscale phenomena

Large regional-scale organization of surface currents, SST, SSS and primary production was observed to be strongly distorted by meanders and smaller scale phenomena under the influence of horizontal advection from highly variable currents. The similarity of

Accepted manuscript

temperature and salinity variations suggested the action of advection processes in modifying salt and temperature at small scales. Numerous processes such as upwellings, mesoscale (20-100 km, Lévy, 2008) eddies and submesoscale (2-20 km) fronts were observed influencing the biological distributions in complex manners.

In the south/south-westward flowing the ALIS currents observed during the Nectalis cruises along the west coast of New Caledonia (Marchesiello et al., 2010), an example of coastal upwelling was observed at stations 1 and 2 during the two seasons. This coastal upwelling was characterized by cool temperatures and high salinities observed to be homogeneous down to 100 m during the cool season and down to 50 m during the hot season. During the cool season the upwelling was also characterized by a shallow nutricline, enhanced chlorophyll at the surface and higher proportion of large phytoplankton cells, which were not observed during the hot season. A coastal upwelling induced by south-east trade winds particularly during the hot season has been reported in a number of other studies (Ganachaud et al., 2010; Marchesiello et al., 2010).

Observations during each season described quite turbulent ocean circulation with myriads of small cyclonic and anticyclonic eddies of ~50-100 km in size. Such observations have also been reported by Chelton et al. (2011b).

The region is known for its strong interactions between the SEC, which enters from the east, the STCC flowing from the west and the tortuous topography of island masses and ocean floor ridges. These interactions between the large scale currents and topography produce non-linearities in the ocean currents (Couvelard et al., 2008; Marchesiello et al., 2010) which can favor eddy developments. Eddies can also be associated with incoming Rossby waves (Killworth et al., 2004) as well as barotropic instabilities resulting from the sheared westward and eastward currents in the northern region of the EEZ (Figure 1). South of ~22°S, Rossby waves and baroclinic instabilities between the surface flowing STCC and the deeper flowing SEC are also known to generate eddy activity as depicted in strong ocean eddy kinetic energy which peaks during the hot season (Qiu et al., 2009).

Accepted manuscript

ACCEPTED MANUSCRIPT

Primary production and phytoplankton composition within eddies can differ depending upon the oceanographic processes and underlying trophic mechanisms operating in time and space. At the mesoscale, cyclonic eddies (southern hemisphere) induces upwellings near eddy centers and "eddy pumping" (Martin and Richards, 2001; McGillicuddy et al., 2007, 1998) of nutrients into the photic layer. Its effects are most commonly observed near eddy centers where enhanced chlorophyll can be found. Conversely in downwelling eddies (anticyclonic in the southern hemisphere) poorer waters are expected.Lateral advection of pre-existing primary production gradients by eddies (Chelton et al., 2011a) or advective concentration/dispersion of floating materials (Dandonneau et al., 2003) are also common mechanisms and linked to mesoscale phenomena. Maximum impacts on phytoplankton are expected at the eddy edge or out of eddies in association with the frontal submesoscale dynamics. Vertical pumping may also occur within submesoscale structures produced by eddy-eddy interactions through frontal and ageostrophic mechanisms (*e.g.* Klein and Lapeyre, 2009; Lévy, 2008).

A number of eddies and frontal oceanographic processes were observed during the Nectalis cruises. The sampling resolution of both *in situ* and satellite data during the Nectalis cruises was sufficient to observe mesoscale eddies (20-100 km scale). However the sampling resolution was insufficient to differentiate between submesoscale fronts (2-20 km scale, Lévy, 2008) and lateral advection.

Enhanced primary production was observed mainly south of ~20°S in the New Caledonia EEZ at the center of several cyclonic eddies (e.g. Nectalis1 eddy A; Nectalis2 eddy D; Nectalis2 eddy G) suggesting the occurrence of eddy pumping. Lower primary production was observed in the downwelling (anticyclonic) eddy at station 9 during Nectalis2 (eddy K). In downwelling areas lateral advection from fluid convergence can concentrate floating organisms (Dandonneau et al. 2003) such as the diazotrophic cyanobacterium *Trichodesmium* which can be quite frequent in the region (Dupouy et al., 2011). At station 9 (Nectalis 2) a higher proportion of large phytoplankton cells with higher concentration of phycoerythrin suggested the presence of *Trichodesmium*, consistent with lateral advection accumulation.

Accepted manuscript

ACCEPTED MANUSCRIPT

Enhanced primary production and chlorophyll were observed more commonly at the edge of several eddies to the north of ~20°S in the more oligotrophic regions. Enhanced primary productivity may have resulted from chlorophyll advected into the area either from the north via a series of cyclonic eddies (e.g. Nectalis2 series of cyclonic eddies H, I, J; Nectalis1 station 10 eddy C) or from the south (Nectalis1 stations 6-7 eddy B). The increased proportion of larger phytoplankton cells at Nectalis1 station 10 (eddy C) is consistent with evolution in composition of eddies with time. The phytoplankton community may have developed in the north and aged along the eddy streamlines as it was advected to the south by eddy currents. However this observation was not consistent for all eddies observed with no specific phytoplankton composition observed at some eddies (e.g. Nectalis1 station 6 eddy B).

Overall, the primary production patterns around New Caledonia appeared to be more highly dominated by horizontal advection rather than by vertical processes (direct eddy pumping). The patchy and high frequency signal complicated the general understanding of the ecosystem organization, as is often the case in oligotrophic waters. More generally, how mesoscale eddies and the submesoscale structures affect primary production is still under debate (Chelton et al., 2011a; Gruber et al., 2011; Klein and Lapeyre, 2009; Lévy, 2008) and the Nectalis data suggests that there is not one particular mechanism at work during the period of the cruises in this region of the South Pacific.

The effect of primary production dynamics at these scales on upper trophic levels are also poorly understood because of the difficulty of accessing datasets spanning a wide range of trophic levels at the scales relevant to eddies and submesoscale structures. Similarly to primary production, the few examples of zooplankton organization around eddies (e.g. Lebourges-Dhaussy et al., 2014; Menkes et al., 2002; Roman et al., 1995) show a variety of organizations. The S-ADCP backscatter (not shown), EK60 Sv and SEAPODYM micronekton data showed strong patchiness, especially in the south, indicating the influence of mesoscale features on the organization of zooplankton and micronekton. Similarly to zooplankton, the relationship between mesoscale features and micronekton distribution is

Accepted manuscript

ACCEPTED MANUSCRIPT

considered to be complex and not yet well understood (Béhagle et al., 2014; Domokos, 2009; Potier et al., 2014).

4.3 Seasonality

Observations collected during the Nectalis cruises reflected strong seasonality in hydrodynamics and water column characteristics in response to the seasonal migration of the solar heating and convective system of the SPCZ. The hot season was characterized by warmer and fresher ocean conditions, increased eddy activity, lower NPP and phytoplankton biomass, and higher stratification as modelled by Marchesiello et al. (2010), The cool season was characterized by lower eddy activity, higher NPP and phytoplankton biomass. The NPP latitudinal gradient during the cool season mimicked the SST gradient, indicating a tight coupling between ocean dynamics and phytoplankton growth. There was a stronger decoupling between the surface temperature patterns and primary production during the hot season, as expected in oligotrophic waters (Le Borgne et al., 2011).

Primary production almost doubled during the cool season compared to the hot season. Contradictory seasonal signals for zooplankton and micronekton biomass, however were provided by various sampling methods, resulting in an inability to determine seasonality in mid-level organisms. Two hypotheses, possibly acting in combination, may explain the observations. Firstly, enhanced net primary production during the cool season may have been largely due to enhanced recycling, with a small portion of the primary production transmitted to higher trophic levels. Secondly, different turn-over times between phytoplankton and zooplankton/micronekton may have induced a time decoupling and a delay in transmission of primary production to secondary and tertiary levels.

It should be noted that, at the time of the cruises in 2011, the South Pacific was considered to be in a weak La Niña state (http://iri.columbia.edu/climate/ENSO/currentinfo/archive/201110/technical.html). In the New Caledonia region, the expected response of the ocean to La Niña is a weakening of the trade winds during the hot season and slightly warmer SST conditions (~+0.5°C in average)

Accepted manuscript

with a slightly deeper thermocline (Menkes, 2012). This weak effect of ENSO in the New Caledonian area however, is unlikely to bias the seasonal view from the two cruises.

4.4 Diel migration

Classical diel behavior of organisms migrating towards the surface at night and to deep waters during the day was observed in both zooplankton and micronekton using acoustic methods. Using net sampling however, the day-night difference in zooplankton DW was not observed in the zooplankton WW for the 0-200 m depth during the hot season. This may be explained by the increase of gelatinous organisms (mainly salps and doliolids) at the surface during the hot season (H. Smeti, *pers. com.*) and their representation in WW and DW estimates. Because gelatinous organisms comprise the largest group in WW estimates, their diel behavior will dominate any diel signal for zooplankton. As they rarely migrate vertically, little day-night differences in WW would be expected for zooplankton. The proportion of DW biomass contributed by gelatinous organisms however is much smaller. The predominance of diel vertical behavior in the other taxa groups then results in a diel signal being evident in zooplankton DW.

4.5 Measuring primary production, zooplankton and micronekton

Despite the high variability observed in our primary production *in situ* measurements, particularly during the cool season, and despite their small number (12 measures out of 41 stations for both cruises), we estimated they were reasonably representative of the entire cruise. *In situ* measures of primary production during both Nectalis cruises were similar to previous studies in the region (300 – 1000 mgC m^{-2} day^{-1} in September 2004 at 28°S and ~155°E-162°E according to Young et al. (2011). These *in situ* measurements were also in the range of values estimated by satellite for the season, providing some validation and allowing confidence in using the satellite VGPM values for a larger scale assessment of primary production.

The biomass estimates of microzooplankton and mesozooplankton (~20-2000 µm) provided by the S-ADCP were significantly correlated to the estimates using acoustics (TAPS) and nets. Estimates derived from the S-ADCP however, are likely to include other organisms and

Accepted manuscript

ACCEPTED MANUSCRIPT

therefore the S-ADCP provides a proxy which is not only reflective of zooplankton biomass (e.g. Burd and Thomson, 2012; Chereskin and Tarling, 2007). The strong correlation between the 153kHz S-ADCP Sv and the EK60 signal, the frequencies of which detect a range of organisms from zooplankton to micronekton and larger, indicate that estimates provided by the S-ADCP also include estimates of micronekton biomass. Although the results did not allow us to define precisely which size-range of organisms was detected by the S-ADCP, and despite the difficulties in calibrating the S-ADCP onboard vessels (Gostiaux and van Haren, 2010), our results suggest that this instrument may provide a useful proxy of relative biomass of zooplankton and micronekton confirming its use as a functional tool for this purpose (Brierley et al., 1998; Flagg and Smith, 1989; Heywood et al., 1991; Lee et al., 2008; Radenac et al., 2010). Given that the S-ADCP has been used routinely for more than two decades to sample ocean currents, the data provided by these instruments could potentially be useful for mapping zooplankton/micronekton biomass distributions.

Correlations between net and acoustic (TAPS) estimates of zooplankton biomass observed in this study have also previously been observed (e.g. Lebourges-Dhaussy et al., 2014; 2009a). Preliminary comparisons between the target micronekton trawls and the EK60 acoustic signal however, were not correlated. These data need to be further explored. Low but significant correlations between micronekton net sampling and acoustic EK60 Sv have previously been found for micronekton south of New Caledonia using standardized oblique tows from 600 m to the surface at night (Young et al., 2011). Net sampling at targeted depth and selectivity/catchability/avoidance biases are some of the classic issues that may explain the often low correlation between micronekton net sampling and acoustic estimates (Kloser et al., 2009; Koslow et al., 1997).

Zooplankton biomass estimates provided by the TAPS were observed to be more than one order of magnitude higher than the biomass estimates provided by net sampling. These results are at odds with previous comparisons in other regions (e.g. Lebourges-Dhaussy et al., 2014, 2009) and at present we do not have a clear explanation for this discrepancy. Several hypotheses can be proposed which might explain such a disagreement. The TAPS detects organisms in the 50-3000 µm size range, while the nets used during the cruises only

Accepted manuscript

ACCEPTED MANUSCRIPT

collected organisms larger than 200 µm. The smaller sized organisms detected by the TAPS but not collected by the net may lead to smaller biomass estimates from net samples. Exploration of the data suggested that differences in the size ranges sampled by each method cannot explain the large difference in the two estimates. A plausible explanation could be the inadequacy of the parameterization of the model used in the inversion algorithm to calculate biomass from the TAPS signal. This would induce an overestimation of the biovolume by the TAPS if, for example, the density contrast between organisms and the water is underestimated. Further exploration of both the data and sampling of the water column by the TAPS is required. Moreover, vertical net sampling of the water column may be insufficient for representatively sample the oligotrophic waters around New Caledonia as the quantity of zooplankton collected was very low. Additional cruises are needed in which alternative sampling methods such as oblique tows which filter larger quantities of water and collect larger quantities of samples can be trialed and investigated.

Biomass estimates of micronekton provided by net sampling and those provided by the SEAPODYM ecosystem model were observed to be in the same range. Because the net sampled at specific depths thereby providing estimates which were not representative of the whole water column, and because of the relative simplicity of the way in which micronekton are estimated in SEAPODYM (Lehodey et al., 2010) this was not necessarily expected. Additionally, micronekton biomass estimates provided by SEAPODYM were significantly correlated to the 38 kHz EK60 acoustic signal. Again this was not expected as the ocean currents used to force SEAPODYM and determine micronekton spatial distribution in the sub-model come from a model reanalysis and not observations. Hence good space/time coherence between observed and modeled mesoscale structures at the time of the observations would not necessarily be expected. Given that the SEAPODYM simulation is simply eddy permitting, these results are encouraging and indicate that the influence of mesoscale features on micronekton biomass is adequately captured by SEAPODYM in this region.

Accepted manuscript

4.6 A broader view of the south-west Pacific

The correlations observed between observations and both VGPM satellite-derived primary production and SEAPODYM estimates of micronekton biomass provide some confidence in using these products in describing the ocean dynamics of the broader south-west Pacific Ocean (~15°S-35°S and 150°E-175°E) encompassing the Coral Sea.

Looking more broadly than the region in which the cruises were conducted, horizontal advections also shaped the horizontal structure of primary production in the. (Figure 9). Using VGPM satellite-derived primary production data and SEAPODYM micronekton estimates, higher primary production and micronekton values were observed south of 23°S during the cool season and south of 31°S during the hot season than areas further north. Across the overall south west Pacific Ocean region, primary production was much stronger (by approximately a factor 2 to 3) during the cool season compared to the hot season as the SPCZ regime weakened and stronger winds promoted replenishment of surface nutrients (Figure 9). A similar seasonal signal was observed in micronekton biomass as derived from SEAPODYM however, the contrast between seasons was smaller than that observed in primary production estimates (micronekton was higher during the cool season by a factor <2).

Micronekton biomass south of 20°S as provided by SEAPODYM was globally organized in very patchy structures and the primary production maxima provided via remote sensing did not necessarily match the micronekton maxima. One good example can be found in the "downwelling"anticylonic eddy in the EAC at 32°S-155°E, where primary production was organized in a strong band around the eddy whereas micronekton biomass was organized along a filament at the edge of the eddy. Estimates of micronekton biomass provided by SEAPODYM indicated that the southern region was richer in biomass, but was also much more variable than the northern region (Figure 9).

Presence of patchy structures and decoupling between different trophic levels raises uncertainty associated with using snapshot surveys to understand the coherence of an

Accepted manuscript

ACCEPTED MANUSCRIPT

ecosystem in turbulent regions. Additional observations in the region will be needed to confirm the nature of the ecosystem organization at (sub) mesoscales.

5 Conclusions and perspectives

By collecting new data extending from the ocean dynamics to micronekton in the top 600 m, the two Nectalis cruises conducted in the south-west Pacific Ocean in austral cool and hot season of 2011 have provided a better understanding of the pelagic offshore ecosystem of this oligotrophic region. Multiple methods were used to measure zooplankton and micronekton (S-ADCP, TAPS, zooplankton net, SIMRAD EK60, micronekton net). Correlations were found between methods, however, net biomass estimates and acoustic-derived estimates did not compare very well. On the other hand, estimates of micronekton provided from net sampling and SEAPODYM were in the same range. The S-ADCP reproduced adequately the trends observed in micronekton and zooplankton, but was unable to distinguish zooplankton from micronekton and absolute biomasses could therefore not be calculated. Calibration of the different methods used to estimate zooplankton and micronekton will require additional and more specifically designed studies. Based on large existing S-ADCP datasets, the demonstrated relation between the S-ADCP signal and the zooplankton/micronekton biomass estimates provides the opportunity to estimate relative zooplankton/micronekton biomasses on much larger scales than those available from dedicated instruments such as EK60 or TAPS. Such effort will be undertaken in the New Caledonia region using the available S-ADCP database spanning the past 20 years. In line with this work, we believe that the development of on-board calibration methods for the S-ADCP similar to those for echosounders (e.g. EK60) would be of great interest, particularly in providing absolute measures of abundance. Models such as SEAPODYM would benefit from absolute biomasses to better calibrate energy transfer parameterizations.

Based on our limited dataset and the resolution of our data, we could not examine the systematic effects of submesoscale phenomenon such as eddies and fronts on ocean

Accepted manuscript

ACCEPTED MANUSCRIPT

biochemistry and planktonic/nektonic communities structures during the Nectalis cruises. Data collected however, did suggest that horizontal advection was dominant over eddy pumping. Our study highlights the difficulty of understanding the impact of eddies in oligotrophic conditions without a full three dimensional dataset. We were also unable to explore the role that spatial variability might have at the submesoscale (frontal) level, a scale at which ecosystems have been shown to organize in some cases (e.g. Lebourges-Dhaussy et al., 2014; Lévy et al., 2012; Tew Kai et al., 2009). This remains an open question of wide scientific interest. Further, two cruises in two seasons are not sufficient to fully describe the role of seasonality on the ecosystem. Additional *in situ* measurements will be required to further understand the magnitude of the spatial distribution and seasonal cycle of zooplankton/micronekton biomass in the region, as planned in the coming years within the framework of the Nectalis program.

The synoptic Nectalis cruises and the SEAPODYM model at the regional scale indicated that the micronekton structure south of 20°S was remarkably patchy during both seasons in relation to the mesoscale dynamics of the region. This patchiness raises the question of how to best sample the region with dedicated cruises. At present, we have chosen to broadly sample the New Caledonian EEZ. We believe that given the large uncertainty in understanding of the ecosystem organization and species, it is still useful to pursue this effort and will be carried out in a series of two additional cruises in the coming years. We also do note that is it extremely difficult to interpret ecosystem signals at the mesoscale level using transects organized to cover wide spatial areas. We therefore aim to design dedicated cruises to follow a number of eddies in the region and understand the time dynamics of such evolving systems.

Accepted manuscript

Acknowledgements

This research was co-funded by the Institute of Research for Development (IRD), the LEFE-CYBER program, the Agence des Aires Marines Protégées (AAMP) and the New Caledonian Zone Economique de Nouvelle-Caledonie (ZoNeCo) program. H. Smeti received support

ACCEPTED MANUSCRIPT

from IRD through its PhD. scholarship program. B. Hunt was supported by a Marie Curie Fellowship (ISOZOO) of the 7th International Framework Programme. V. Allain was supported by the Australian Overseas Aid Program (AUSAID). We thank Magali Teurlai (IRD, UMR LOCEAN/UMR ESPACE-DEV) for guidance on statistical analyses, Aude Barani (PRECYM) for analyses as well as Philippe Gérard (IRD, US LAMA). We are grateful to the captain, Jean-François Barazer (IRD), and the crew of the R/V Alis for their work during the cruises, to Yves Gouriou (IRD) for the preparation of the cruises, to Elodie Vourey (SPC) and Jeff Dubosc (SPC) for their assistance with identification of micronekton organisms. We also thank the two anonymous reviewers and Karen Evans (CSIRO) whose comments significantly improved this manuscript.

Accepted manuscript

References

Abecassis, M., Senina, I., Lehodey, P., Gaspar, P., Parker, D., Balazs, G., Polovina, J., 2013. A model of loggerhead sea turtle (*Caretta caretta*) habitat and movement in the oceanic North Pacific. PLoS ONE 8, e73274. doi:10.1371/journal.pone.0073274

Allain, V., Fernandez, E., Hoyle, S.D., Caillot, S., Jurado-Molina, J., Andréfouët, S., Nicol, S.J., 2012. Interaction between coastal and oceanic ecosystems of the Western and Central Pacific Ocean through predator-prey relationship studies. PLos ONE 7, e36701.

Aminot, A., Kérouel, R., 2007. Dosage automatique des nutriments dans les eaux marines: méthodes en flux continu. IFREMER, Paris.

Barnier, B., Madec, G., Penduff, T., Molines, J.-M., Treguier, A.-M., Sommer, J.L., Beckmann, A., Biastoch, A., Böning, C., Dengg, J., Derval, C., Durand, E., Gulev, S., Remy, E., Talandier, C., Theetten, S., Maltrud, M., McClean, J., Cuevas, B.D., 2006. Impact of partial steps and momentum advection schemes in a global ocean circulation model at eddy-permitting resolution. Ocean Dyn. 56, 543–567. doi:10.1007/s10236-006-0082-1

Béhagle, N., du Buisson, L., Josse, E., Lebourges-Dhaussy, A., Roudaut, G., Ménard, F., 2014. Mesoscale features and micronekton in the Mozambique Channel: An acoustic approach. Deep Sea Res. Part II 100, 164–173. doi:10.1016/j.dsr2.2013.10.024

Behrenfeld, M., Falkowski, P.G., 1997. A consumer's guide to phytoplankton primary productivity models. Limnol. Oceanogr. 42, 1479–1491. doi:10.4319/lo.1997.42.7.1479

Bell, J.D., Reid, C., Batty, M.J., Lehodey, P., Rodwell, L., Hobday, A.J., Johnson, J.E., Demmke, A., 2013. Effects of climate change on oceanic fisheries in the tropical Pacific: implications for economic development and food security. Clim. Change 119, 199–212. doi:10.1007/s10584-012-0606-2

Bertrand, A., Le Borgne, R., Josse, E., 1999. Acoustic characterisation of micronekton distribution in French Polynesia. Mar. Ecol. Prog. Ser. 191, 127–140.

Briand, K., Molony, B., Lehodey, P., 2011. A study on the variability of albacore (*Thunnus alalunga*) longline catch rates in the southwest Pacific Ocean. Fish. Oceanogr. 20, 517–529. doi:10.1111/j.1365-2419.2011.00599.x

Brierley, A.S., Brandon, M.A., Watkins, J.L., 1998. An assessment of the utility of an acoustic Doppler current profiler for biomass estimation. Deep Sea Res. Part I 45, 1555–1573. doi:10.1016/S0967-0637(98)00012-0

Burd, B., Thomson, R., 2012. Estimating zooplankton biomass distribution in the water column near the endeavour segment of Juan de Fuca Ridge using acoustic backscatter and concurrently towed nets. Oceanography 25, 269–276. doi:10.5670/oceanog.2012.25

Campbell, L., Carpenter, E.J., Montoya, J.P., Kustka, A.B., Capone, D.G., 2005. Picoplankton community structure within and outside a *Trichodesmium* bloom in the southwestern Pacific Ocean. Life Environ. 55, 185–195.

Carassou, L., Le Borgne, R., Rolland, E., Ponton, D., 2010. Spatial and temporal distribution of zooplankton related to the environmental conditions in the coral reef lagoon of

Accepted manuscript

New Caledonia, Southwest Pacific. Mar. Pollut. Bull. 61, 367–374. doi:10.1016/j.marpolbul.2010.06.016

Ceccarelli, D.M., McKinnon, A.D., Andréfouët, S., Allain, V., Young, J., Gledhill, D.C., Flynn, A., Bax, N.J., Beaman, R., Borsa, P., Brinkman, R., Bustamante, R.H., Campbell, R., Cappo, M., Cravatte, S., D’Agata, S., Dichmont, C.M., Dunstan, P.K., Dupouy, C., Edgar, G., Farman, R., Furnas, M., Garrigue, C., Hutton, T., Kulbicki, M., Letourneur, Y., Lindsay, D., Menkes, C., Mouillot, D., Parravicini, V., Payri, C., Pelletier, B., Richer de Forges, B., Ridgway, K., Rodier, M., Samadi, S., Schoeman, D., Skewes, T., Swearer, S., Vigliola, L., Wantiez, L., Williams, A., Williams, A., Richardson, A.J., 2013. The Coral Sea: physical environment, ecosystem status and biodiversity assets, in: Michael Lesser (Ed.), Advances in Marine Biology. Academic Press, pp. 213–290.

Chelton, D.B., Gaube, P., Schlax, M.G., Early, J.J., Samelson, R.M., 2011a. The influence of nonlinear mesoscale eddies on near-surface oceanic chlorophyll. Science 334, 328–332. doi:10.1126/science.1208897

Chelton, D.B., Schlax, M.G., Samelson, R.M., 2011b. Global observations of nonlinear mesoscale eddies. Prog. Oceanogr. 91, 167–216. doi:10.1016/j.pocean.2011.01.002

Chereskin, T.K., Tarling, G.A., 2007. Interannual to diurnal variability in the near-surface scattering layer in Drake Passage. ICES J Mar Sci 64, 1617–1626.

Couvelard, X., Marchesiello, P., Gourdeau, L., Lefèvre, J., 2008. Barotropic zonal jets induced by islands in the Southwest Pacific. J. Phys. Oceanogr. 38, 2185–2204. doi:10.1175/2008JPO3903.1

D’ Ovidio, F., De Monte, S., Penna, A.D., Cotté, C., Guinet, C., 2013. Ecological implications of eddy retention in the open ocean: a Lagrangian approach. J. Phys. Math. Theor. 46, 254023. doi:10.1088/1751-8113/46/25/254023

Dandonneau, Y., Gohin, F., 1984. Meridional and seasonal variations of the sea surface chlorophyll concentration in the southwestern tropical Pacific (14 to 32°S, 160 to 175°E). Deep Sea Res. Part A 31, 1377–1393. doi:10.1016/0198-0149(84)90078-5

Dandonneau, Y., Vega, A., Loisel, H., Penhoat, Y. du, Menkes, C., 2003. Oceanic Rossby waves acting as a “hay rake” for ecosystem floating by-products. Science 302, 1548–1551. doi:10.1126/science.1090729

De Boyer Montégut, C., Madec, G., Fischer, A.S., Lazar, A., Iudicone, D., 2004. Mixed layer depth over the global ocean: An examination of profile data and a profile-based climatology. J. Geophys. Res. Oceans 109, C12003. doi:10.1029/2004JC002378

Deines, K.L., 1999. Backscatter estimation using Broadband acoustic Doppler current profilers, in: Anderson, S.P., Terray, E.A., Rizoli White, J.A., Williams 3rd, A.J. (Eds.), Proceedings of the IEEE Sixth Working Conference on Current Measurement, 1999. IEEE, Piscataway, pp. 249–253. doi:10.1109/CCM.1999.755249

Domokos, R., 2009. Environmental effects on forage and longline fishery performance for albacore (*Thunnus alalunga*) in the American Samoa Exclusive Economic Zone. Fish. Oceanogr. 18, 419–438.

Dupouy, C., Benielli-Gary, D., Neveux, J., Dandonneau, Y., Westberry, T.K., 2011. An algorithm for detecting Trichodesmium surface blooms in the South Western Tropical Pacific. Biogeosciences 8, 3631–3647. doi:10.5194/bg-8-3631-2011

Accepted manuscript

Dutrieux, P., Menkes, C.E., Vialard, J., Flament, P., Blanke, B., 2008. Lagrangian study of tropical instability vortices in the Atlantic. J. Phys. Oceanogr. 38, 400–417. doi:10.1175/2007JPO3763.1

Farley, J.H., Williams, A.J., Hoyle, S.D., Davies, C.R., Nicol, S.J., 2013. Reproductive dynamics and potential annual fecundity of South Pacific albacore tuna (*Thunnus alalunga*). PLoS ONE 8, e60577. doi:10.1371/journal.pone.0060577

Ferry, N., Parent, L., Garric, M., Drevillon, C., Desportes, C., Bricaud, F., Hernandez, F., 2012. Scientific Validation Report (ScVR) for reprocessed analysis and reanalysis. MyOcean Proj. Rep. MYO-WP04-ScCV-Rea-Mercat.-V10 1–66.

Flagg, C.N., Smith, S.L., 1989. On the use of the acoustic doppler current profiler to measure zooplankton abundance. Deep Sea Res. Part A 36, 455–474. doi:10.1016/0198-0149(89)90047-2

Flynn, A.J., Paxton, J.R., 2012. Spawning aggregation of the lanternfish *Diaphus danae* (family Myctophidae) in the north-western Coral Sea and associations with tuna aggregations. Mar. Freshw. Res. 63, 1255–1271.

Foote, K.G., Knudsen, H.P., Vestnes, D.N., MacLennan, D.N., Simmonds, E.J., 1987. Calibration of acoustic instruments for fish density estimation: a practical guide. ICES Coop. Res. Rep. 144.

Ganachaud, A., Vega, A., Rodier, M., Dupouy, C., Maes, C., Marchesiello, P., Eldin, G., Ridgway, K., Le Borgne, R., 2010. Observed impact of upwelling events on water properties and biological activity off the southwest coast of New Caledonia. Mar. Pollut. Bull. 61, 449–464. doi:10.1016/j.marpolbul.2010.06.042

Gillett, R., 2009. Fisheries in the economies of the Pacific island countries and territories. Asian Development Bank, Mandaluyong City.

Gostiaux, L., van Haren, H., 2010. Extracting meaningful information from uncalibrated backscattered echo intensity data. J. Atmospheric Ocean. Technol. 27, 943–949. doi:10.1175/2009JTECHO704.1

Gourdeau, L., Kessler, W.S., Davis, R.E., Sherman, J., Maes, C., Kestenare, E., 2008. Zonal jets entering the Coral Sea. J. Phys. Oceanogr. 38, 715–725. doi:10.1175/2007JPO3780.1

Grandperrin, R., 1969. Couches diffusantes dans le Pacifique équatorial et sud-tropical. Cah. ORSTOM Sér. Océan. VII, 99–112.

Grandperrin, R., 1975. Structures trophiques aboutissant aux thons de longue ligne dans le Pacifique sud-ouest tropical. Thèse Détat Univ. Aix-Marseille II 1–296.

Gruber, N., Lachkar, Z., Frenzel, H., Marchesiello, P., Münnich, M., McWilliams, J.C., Nagai, T., Plattner, G.-K., 2011. Eddy-induced reduction of biological production in eastern boundary upwelling systems. Nat. Geosci. 4, 787–792. doi:10.1038/ngeo1273

Heywood, K.J., Scrope-Howe, S., Barton, E.D., 1991. Estimation of zooplankton abundance from shipborne ADCP backscatter. Deep Sea Res. Part A 38, 677–691. doi:10.1016/0198-0149(91)90006-2

Holliday, D.V., Pieper, R.E., 1980. Volume scattering strengths and zooplankton distributions at acoustic frequencies between 0.5 and 3 MHz. J. Acoust. Soc. Am. 135–146.

Holliday, D.V., Pieper, R.E., Kleppel, G.S., 1989. Determination of zooplankton size and distribution with multifrequency acoustic technology. ICES J. Mar. Sci. 46, 52–61. doi:10.1093/icesjms/46.1.52

Accepted manuscript

ACCEPTED MANUSCRIPT

Hummon, J.M., Firing, E., 2003. A direct comparison of two RDI shipboard ADCPs: a 75-kHz ocean surveyor and a 150-kHz narrow band. J. Atmospheric Ocean. Technol. 20, 872–888.

Hunt, B.P.V., Allain, V., Lorrain, A., Menkes, C., Rodier, M., Pagano, M., Carlotti, F., Graham, B.S., this issue. Size-structured interactions in a sub-tropical pelagic food web. Deep Sea Res. Part II.

Hydro-Bios Apparatebau GmbH, 2009. Multi plankton sampler Multinet Type Midi. Operation manual. Hydro-Bios Apparatebau GmbH, Kiel-Altenholz.

Jacquet, S., Delesalle, B., Torrton, J., Blanchot, J., 2006. Response of phytoplankton communities to increased anthropogenic influences (southwestern lagoon, New Caledonia). Mar. Ecol. Prog. Ser. 320, 65–78. doi:10.3354/meps320065

Kessler, W.S., Cravatte, S., 2013. Mean circulation of the Coral Sea. J. Geophys. Res. Oceans 118, 6385–6410. doi:10.1002/2013JC009117

Killworth, P.D., Cipollini, P., Uz, B.M., Blundell, J.R., 2004. Physical and biological mechanisms for planetary waves observed in satellite-derived chlorophyll. J. Geophys. Res. Oceans 109, C07002. doi:10.1029/2003JC001768

Klein, P., Lapeyre, G., 2009. The oceanic vertical pump induced by mesoscale and submesoscale turbulence. Annu. Rev. Mar. Sci. 1, 351–375. doi:10.1146/annurev.marine.010908.163704

Kloser, R., Ryan, T., Young, J.W., Lewis, M.E., 2009. Acoustic observations of micronekton fish on the scale of an ocean basin: potential and challenges. ICES J. Mar. Sci. 66, 998–1006.

Koslow, J.A., Kloser, R.J., Williams, A., 1997. Pelagic biomass and community structure over the mid-continental slope off southeastern Australia based upon acoustic and midwater trawl sampling. Mar. Ecol.-Prog. Ser. 146, 21–35. doi:10.3354/meps146021

Le Borgne, R., Allain, V., Matear, R.J., Griffiths, S.P., McKinnon, A.D., Richardson, A.J., Young, J.W., 2011. Vulnerability of open ocean food webs in the tropical Pacific to climate change, in: Bell, J., Johnson, J.E., Hobday, A.J. (Eds.), Vulnerability of Fisheries and Aquaculture in the Tropical Pacific to Climate Change. Secretariat of the Pacific Community, Noumea, pp. 189–250.

Le Bouteiller, A., Blanchot, J., Rodier, M., 1992. Size distribution patterns of phytoplankton in the western Pacific: towards a generalization for the tropical open ocean. Deep Sea Res. Part A 39, 805–823. doi:10.1016/0198-0149(92)90123-B

Lebourges-Dhaussy, A., Coetzee, J., Hutchings, L., Roudaut, G., Nieuwenhuys, C., 2009. Zooplankton spatial distribution along the South African coast studied by multifrequency acoustics, and its relationships with environmental parameters and anchovy distribution. ICES J. Mar. Sci. 66, 1055–1062. doi:10.1093/icesjms/fsp129

Lebourges-Dhaussy, A., Huggett, J., Ockhuis, S., Roudaut, G., Josse, E., Verheye, H., 2014. Zooplankton size and distribution within mesoscale structures in the Mozambique Channel: A comparative approach using the TAPS acoustic profiler, a multiple net sampler and ZooScan image analysis. Deep Sea Res. Part II 100, 136–152. doi:10.1016/j.dsr2.2013.10.022

Accepted manuscript

ACCEPTED MANUSCRIPT

Lee, K., Mukai, T., Lee, D., Iida, K., 2008. Verification of mean volume backscattering strength obtained from acoustic doppler current profiler by using sound scattering layer. Fish. Sci. 74, 221–229. doi:10.1111/j.1444-2906.2008.01516.x

Legand, M., Bourret, P., Grandperrin, R., Rivaton, J., 1970. A preliminary study of some micronektonic fishes in the equatorial and tropical western Pacific, in: Scientific Exploration of the South Pacific. National Academy of sciences, Washington,D.C., pp. 225–235.

Lehodey, P., Andre, J.-M., Bertignac, M., Hampton, J., Stoens, A., Menkes, C., Memery, L., Grima, N., 1998. Predicting skipjack tuna forage distributions in the equatorial Pacific using a coupled dynamical bio-geochemical model. Fish. Oceanogr. 7, 317–325. doi:10.1046/j.1365-2419.1998.00063.x

Lehodey, P., Murtugudde, R., Senina, I., 2010. Bridging the gap from ocean models to population dynamics of large marine predators: a model of mid-trophic functional groups. Prog. Oceanogr. 84, 69–84.

Lehodey, P., Senina, I., Murtugudde, R., 2008. A spatial ecosystem and populations dynamics model (SEAPODYM) – Modeling of tuna and tuna-like populations. Prog. Oceanogr. 78, 304–318. doi:10.1016/j.pocean.2008.06.004

Lévy, M., 2008. The modulation of biological production by oceanic mesoscale turbulence, in: Weiss, J.B., Provenzale, A. (Eds.), Transport and Mixing in Geophysical Flows. Springer Berlin Heidelberg, pp. 219–261.

Lévy, M., Ferrari, R., Franks, P.J.S., Martin, A.P., Rivière, P., 2012. Bringing physics to life at the submesoscale. Geophys. Res. Lett. 39, L14602. doi:10.1029/2012GL052756

MacLennan, D.N., Fernandes, P.G., Dalen, J., 2002. A consistent approach to definitions and symbols in fisheries acoustics. ICES J. Mar. Sci. 59, 365–369. doi:10.1006/jmsc.2001.1158

Marchesiello, P., Lefèvre, J., Vega, A., Couvelard, X., Menkes, C., 2010. Coastal upwelling, circulation and heat balance around New Caledonia's barrier reef. Mar. Pollut. Bull. 61, 432–448. doi:10.1016/j.marpolbul.2010.06.043

Martin, A.P., Richards, K.J., 2001. Mechanisms for vertical nutrient transport within a North Atlantic mesoscale eddy. Deep Sea Res. Part II 48, 757–773. doi:10.1016/S0967-0645(00)00096-5

McClatchie, S., Dunford, A., 2003. Estimated biomass of vertically migrating mesopelagic fish off New Zealand. Deep Sea Res. Part I 50, 1263–1281. doi:10.1016/S0967-0637(03)00128-6

McGillicuddy, D.J., Anderson, L.A., Bates, N.R., Bibby, T., Buesseler, K.O., Carlson, C.A., Davis, C.S., Ewart, C., Falkowski, P.G., Goldthwait, S.A., Hansell, D.A., Jenkins, W.J., Johnson, R., Kosnyrev, V.K., Ledwell, J.R., Li, Q.P., Siegel, D.A., Steinberg, D.K., 2007. Eddy/wind interactions stimulate extraordinary mid-ocean plankton blooms. Science 316, 1021–1026. doi:10.1126/science.1136256

McGillicuddy, D.J., Robinson, A.R., Siegel, D.A., Jannasch, H.W., Johnson, R., Dickey, T.D., McNeil, J., Michaels, A.F., Knap, A.H., 1998. Influence of mesoscale eddies on new production in the Sargasso Sea. Nature 394, 263–266. doi:10.1038/28367

McKinnon, A.D., 2005. Mesozooplankton dynamics in nearshore waters of the Great Barrier Reef. Estuar. Coast. Shelf Sci. 497–511. doi:10.1016/j.ecss.2004.12.011

Accepted manuscript

McPherson, G.R., 1991. A possible mechanism for the aggregation of yellowfin and bigeye tuna in the north-western Coral Sea. Queensland Department of Primary Industries - Information Series. QI91013, 1–11.

Menkes, C., 2012. Les grandes fluctuations des hydroclimats : le phénomène ENSO, in: Bonvallot, J., Gay, J.-C., Habert, E. (Eds.), Atlas de la Nouvelle Calédonie. IRD, Marseille, pp. 49–52.

Menkes, C.E., Kennan, S.C., Flament, P., Dandonneau, Y., Masson, S., Biessy, B., Marchal, E., Eldin, G., Grelet, J., Montel, Y., Morlière, A., Lebourges-Dhaussy, A., Moulin, C., Champalbert, G., Herbland, A., 2002. A whirling ecosystem in the equatorial Atlantic. Geophys.Res.Lett. 29, 1553.

Moutin, T., Broeck, N.V.D., Beker, B., Dupouy, C., Rimmelin, P., Bouteiller, A.L., 2005. Phosphate availability controls *Trichodesmium spp.* biomass in the SW Pacific Ocean. Mar. Ecol. Prog. Ser. 297, 15–21. doi:10.3354/meps297015

Murphy, J., Riley, J.P., 1962. A modified single solution method for the determination of phosphate in natural waters. Anal. Chim. Acta 27, 31–36. doi:10.1016/S0003-2670(00)88444-5

Napp, J.M., Ortner, P.B., Pieper, R.E., Holliday, D.V., 1993. Biovolume-size spectra of epipelagic zooplankton using a multi-frequency acoustic profiling system (MAPS). Deep Sea Res. Part I 40, 445–459. doi:10.1016/0967-0637(93)90141-O

Neveux, J., Tenorio, M.M.B., Jacquet, S., Torreton, J.-P., Douillet, P., Ouillon, S., Dupouy, C., 2009. Chlorophylls and phycoerythrins as markers of environmental forcings including cyclone Erica effect (March 2003) on phytoplankton in the Southwest lagoon of New Caledonia and oceanic adjacent area. Int. J. Oceanogr. 2009 (Article ID 232513), 19p. doi:10.1155/2009/232513

Olson, R.J., Duffy, L.M., Kuhnert, P.M., Galván-Magaña, F., Bocanegra-Castillo, N., Alatorre-Ramírez, V., 2014. Decadal diet shift in yellowfin tuna (*Thunnus albacares*) suggests broad-scale food web changes in the eastern tropical Pacific Ocean. Mar. Ecol. Prog. Ser. 497, 157–178.

Pieper, R.E., Holliday, D.V., Kleppel, G.S., 1990. Quantitative zooplankton distributions from multifrequency acoustics. J. Plankton Res. 12, 433–441. doi:10.1093/plankt/12.2.433

Pieper, R.E., McGehee, D.E., Greenlaw, C.F., Holliday, D.V., 2001. Acoustically measured seasonal patterns of Zooplankton in the Arabian Sea. Deep Sea Res. Part II 48, 1325–1343. doi:10.1016/S0967-0645(00)00141-7

Potier, M., Bach, P., Ménard, F., Marsac, F., 2014. Influence of mesoscale features on micronekton and large pelagic fish communities in the Mozambique Channel. Deep Sea Res. Part II 100, 184–199. doi:10.1016/j.dsr2.2013.10.026

Qiu, B., Chen, S., Kessler, W.S., 2009. Source of the 70-Day mesoscale eddy variability in the Coral Sea and the north Fiji Basin. J. Phys. Oceanogr. 39, 404–420. doi:10.1175/2008JPO3988.1

Qu, T., Lindstrom, E.J., 2002. A climatological interpretation of the circulation in the western South Pacific. J. Phys. Oceanogr. 32, p2492.

Radenac, M.-H., Plimpton, P.E., Lebourges-Dhaussy, A., Commien, L., McPhaden, M.J., 2010. Impact of environmental forcing on the acoustic backscattering strength in the equatorial Pacific: Diurnal, lunar, intraseasonal, and interannual variability. Deep Sea Res. Part I 57, 1314–1328.

Accepted manuscript

Raimbault, P., Slawyk, G., Coste, B., Fry, J., 1990. Feasibility of using an automated colorimetric procedure for the determination of seawater nitrate in the 0 to 100 nM range: examples from field and culture. Mar. Biol. 104, 347–351. doi:10.1007/BF01313277

Ridgway, K., Dunn, J.R., 2003. Mesoscale structure of the mean East Australian Current System and its relationship with topography. Prog. Oceanogr. 189–222. doi:10.1016/S0079-6611(03)00004-1

Ridgway, K.R., Dunn, J.R., Wilkin, J.L., 2002. Ocean interpolation by four-dimensional weighted least squares—application to the waters around Australasia. J. Atmospheric Ocean. Technol. 19, 1357–1375.

RochelleNewall, E.J., Torrton, J.P., Mari, X., Pringault, O., 2008. Phytoplankton-bacterioplankton coupling in a subtropical South Pacific coral reef lagoon. Aquat. Microb. Ecol. 50, 221–229. doi:10.3354/ame01158

Roger, C., 1974. Répartitions bathymétriques et migrations verticales des Euphausiacés (crustacés) dans les zones de pêche au thon du Pacifique sud-tropical. Cah. ORSTOM Sér. Océan. XII, 221–239.

Roger, C., 1986. Macroplancton et micronecton dans le Pacifique Tropical Sud-Ouest. Oceanogr. Trop. 21, 153–165.

Roman, M.R., Dam, H.G., Gauzens, A.L., Urban-Rich, J., Foley, D.G., Dickey, T.D., 1995. Zooplankton variability on the equator at 140°W during the JGOFS EqPac study. Deep Sea Res. Part II 42, 673–693. doi:10.1016/0967-0645(95)00025-L

Rouyer, T., Fromentin, J.-M., Ménard, F., Cazelles, B., Briand, K., Pianet, R., Planque, B., Stenseth, N.C., 2008. Complex interplays among population dynamics, environmental forcing, and exploitation in fisheries. Proc. Natl. Acad. Sci. 105, 5420–5425. doi:10.1073/pnas.0709034105

Senina, I., Sibert, J., Lehodey, P., 2008. Parameter estimation for basin-scale ecosystem-linked population models of large pelagic predators: application to skipjack tuna. Prog. Oceanogr. 78, 319–335.

Simmonds, E.J., MacLennan, D., 2005. Fisheries acoustics theory and practice. Blackwell, Oxford.

Sutor, M.M., Cowles, T.J., Peterson, W.T., Pierce, S.D., 2005. Acoustic observations of finescale zooplankton distributions in the Oregon upwelling region. Deep Sea Res. Part II 52, 109–121. doi:10.1016/j.dsr2.2004.09.029

Tew Kai, E., Rossi, V., Sudre, J., Weimerskirch, H., Lopez, C., Hernandez-Garcia, E., Marsac, F., Garçon, V., 2009. Top marine predators track Lagrangian coherent structures. Proc. Natl. Acad. Sci. 106, 8245–8250. doi:10.1073/pnas.0811034106

Wyman, M., 1992. An in vivo method for the estimation of phycoerythrin concentrations in marine cyanobacteria (*Synechococcus spp.*). Limnol. Oceanogr. 37, 1300–1306.

Young, J.W., Hobday, A.J., Campbell, R.A., Kloser, R.J., Bonham, P.I., Clementson, L.A., Lansdell, M.J., 2011. The biological oceanography of the East Australian Current and surrounding waters in relation to tuna and billfish catches off eastern Australia. Deep Sea Res. Part II 58, 720–733.

Young, J.W., Hunt, B.P.V., Cook, T., Llopiz, J., Hazen, E.L., Pethybridge, H., Ceccarelli, D., Lorrain, A., Olson, R.J., Allain, V., Menkes, C., Patterson, T., Nicol, S., Lehodey, P.,

Accepted manuscript

Kloser, R., Arrizabalaga, H., Choy, C.A., this issue. The trophodynamics of marine top predators: advances and challenges. Deep-Sea Res. Part II.
Young, J.W., Lansdell, M., Campbell, R., Cooper, S., Juanes, F., Guest, M., 2010. Feeding ecology and niche segregation in oceanic top predators off eastern Australia. Mar. Biol. 157, 2347–2368.

Accepted manuscript

Table 1. Summary of the cruise activities.

	Nectalis1	Nectalis2
Number of sampling stations	18	23
Physics:		
Temperature, salinity, fluorescence, oxygen 0-500 m: CTD sensors	All stations	All stations
Currents: 153 kHz ship borne-ADCP (16-200 m)	Along the track	Along the track
Sea surface salinity and temperature: thermosalinograph	Along the track	Along the track
Nutrients:		
Nutrients, NOx, SRP, 8 depths: 180 m, 150 m, 130 m, 90 m, 70 m, 40 m, 3 m; CTD water sampling	All stations	All stations
Phytoplankton & pigments:		
Total Chlorophyll, 8 depths, fluorometry	All stations	All stations
Size fractionated chlorophyll (<3 µm, 3-10 µm, >10 µm): 8 depths, fluorometry	Stations 2, 4, 6, 8, 10, 12, 14, 16	Stations 1, 2, 6, 9, 11, 14, 17, 20, 23
Pigments: Phycoerythrin, 4 depths in the euphotic zone depending of the stratification (3m, between 20-40m, DCM, below DCM) spectrofluorometry.	Every other station	Every other station
Cell counts: CTD water sampling and flow cytometry	Stations 1, 3, 5, 7, 9 11, 13, 14, 15, 17, 18	Stations 1, 3, 5, 7, 9, 11, 15, 17, 19, 21, 23
Primary production:		
3 depths (surface, between 20-40m, DCM), ^{14}C tracer technique	Stations 1, 4, 7, 9, 13, 16, 17	Stations 4,8,12,15, 21
Zooplankton:		
Net sampling: Hydrobios 5 layer (0-600 m) mesh > 200 µm	All stations	All stations
Acoustics: 1 frequency 153 kHz S-ADCP (16-200 m)	Along the track	Along the track
Acoustics: 6 frequency zooplankton profiler TAPS (0-200 m)	All stations	All stations
Micronekton:		
Net sampling: micronekton net between 14 and 540 m depth (10 mm codend mesh size)	All stations	All stations
Acoustics: 4 frequency EK60 SIMRAD echosounder (0-600 m)	Along the track	Along the track
Acoustics: 1 frequency 153 kHz S-ADCP (16-200 m)	Along the track	Along the track

Accepted manuscript

ACCEPTED MANUSCRIPT

Table 2. Mean and standard deviation (SD) of primary production, biomass estimates and acoustic signal of zooplankton and micronekton during the cool season (Nectalis1) and the hot season (Nectalis2). Results of the Mann-Whitney statistical test (for α=5%) comparing Nectalis 1 (N1) and Nectalis2 (N2) and percentage of the number of tests producing this result for datasets with spatial auto-correlation (see section 2.3.1 for detailed explanation). Seasonal difference between micronekton biomass estimates derived from net sampling was not undertaken because different times and depths were sampled during each survey. DW: dry weight; WW: wet weight.

	Nectalis1		Nectalis2		Seasonal difference (Mann-Whitney) and percentage of tests producing the result
	Mean	SD	Mean	SD	
In situ primary production (mgC m^{-2} d^{-1})	352	160	231	133	N1>N2
Satellite derived primary production along the cruise track (mgC m^{-2} d^{-1})	301	62	199	55	100% N1>N2
Sv ADCP (dB)	-82.2	3.5	-83.4	2.8	80% N1>N2; 20% No difference
TAPS biovolume (mg m^{-3})	107.7	37.3	106.7	22.6	No difference
Zooplankton DW. 0-200 m (mg m^{-3})	3.9	2.6	5.8	2.3	N1<N2
Zooplankton WW. 0-600 m (mg m^{-3})	6.3	3.4	5.6	1.8	No difference
Micronekton (net) mg m^{-3})	3.4	3.0	7.1	6.8	
Sv EK60 0-600 m (dB)	-77.8	2.7	-77.7	2.6	No difference at 100%
Micronekton (SEAPODYM 0-600 m mg m^{-3})	4.3	1.2	4.3	0.9	No difference at 100%

Accepted manuscript

ACCEPTED MANUSCRIPT

Table 3. Correlations between estimates of zooplankton biomass derived from each of the sampling methods deployed during the cruises. Grouped Nectalis1 and 2 Spearman's correlations and p-values between zooplankton dry and wet weight measurements (in mg m^{-3}) from net sampling and their acoustic proxies, S-ADCP Sv (in decibels, dB) and TAPS biovolume (in mg m^{-3}) for the averaged top 100 m and top 200 m. Statistics involving S-ADCP Sv is performed by calculating $\log_{10}$ of TAPS biovolume, zooplankton DW and WW.

Variables	Spearman's correlation coefficient		p-value	
	0-100 m	0-200 m	0-100 m	0-200 m
S-ADCP Sv vs. $\log_{10}$(TAPS biovolume)	0.58	0.64	7e-5*	7e-6*
S-ADCP Sv vs. $\log_{10}$(zoopl. dry weight from net)	0.53	0.66	6e-4*	1e-5*
S-ADCP Sv vs. $\log_{10}$(zoopl. wet weight from net)	0.44	0.36	5e-3*	0.03*
TAPS biovolume vs. zoopl. dry weight from net	0.52	0.61	9e-4*	6e-5*
TAPS biovolume vs. zoopl. wet weight from net	0.46	0.55	3e-3*	4e-4*

* significant correlation at 5%

Accepted manuscript

ACCEPTED MANUSCRIPT

Table 4. Correlations between estimates of micronekton biomasses. Grouped Nectalis1 and 2 Spearman's correlations and significance between the four frequencies of S-ADCP Sv (dB) and the corresponding EK60 Sv (dB) averaged across 0-200m, and between estimates derived from $\log_{10}$ (SEAPODYM) and the corresponding 38 kHz EK60 Sv (dB) average across 0-350 m. Statistics involving S-ADCP Sv is performed by calculating $\log_{10}$ of TAPS biovolume, zooplankton DW and WW.

Variables	Range of Spearman's correlation coefficient	Percentage of significant correlations at α=0.05
S-ADCP Sv vs. 200 kHz EK60 Sv	0.83-0.90	100%
S-ADCP Sv vs. 120 kHz EK60 Sv	0.85-0.92	100%
S-ADCP Sv vs. 70 kHz EK60 Sv	0.87-0.96	100%
S-ADCP Sv vs. 38 kHz EK60 Sv	0.73-0.79	100%
Log_{10}(SEAPODYM) vs. 38 kHz EK60 Sv	0.66-0.80	100%

Accepted manuscript

Figures

Figure 1: Mean 1998-2007 primary production estimated from satellite (VGPM) in mgC m^{-2} d^{-1} (shading). Regions of ocean depth shallower than 200 m have been blocked out. Mean depth of the 1 µM nitrate isopleth (proxy for the nitracline depth) was extracted from CARS climatology (http://www.marine.csiro.au/~dunn/cars2009/) (Ridgway et al., 2002) in meters (contour lines) and mean 0-150 meter total geostrophic currents sourced from Kessler and Cravatte (2013) (vectors). The New Caledonia Exclusive Economic Zone is delineated by the white line.

Figure 2: Mean surface *in situ* (left column) and satellite-derived (right column) oceanographic conditions in the New Caledonian region during the cool season (Nectalis1 - 29 July to 16 August 2011): cruise track and station numbers with those sampled at night in bold red and those sampled during the day in regular black (top left); thermosalinograph sea-surface temperature in °C (SST) and salinity (SSS) (middle left); 0-150 m averaged currents in m s^{-1} (vectors) from the S-ADCP with blue and red arrows indicating eastward and westward currents respectively (bottom left); surface currents (vectors) from OSCAR (right column), scale identical to S-ADCP scale; MODIS-VGPM derived depth-integrated net primary production in mgC m^{-2} $d\text{-}^{1}$ (top right); GHRSST satellite sea surface temperature in °C (top-middle right); sea level anomalies (SLA) referenced to the mean geoid in cm (bottom-middle right), letters indicate eddies identified in the text; eddy depiction index: Okubo-Weiß parameter (day^{-2}) (bottom right). The cruise track is plotted in black on the right column.

Figure 3: Mean surface *in situ* (left column) and satellite-derived (right column) oceanographic conditions in the New Caledonian region during the hot season (Nectalis2 - 26 November to 14 December 2011). See Figure 2 caption for details.

Figure 4. Biogeochemical parameters across 0-200 m along cruise tracks during the cool season (Nectalis1, left panel) and the hot season (Nectalis2, right panel), from CTD sensors and bottle water analyses. The x-axis labels denote station numbers. From top to bottom: temperature (°C), salinity, nitrate (NO_3 µM), phosphate (PO_4 µM), chlorophyll (mg m^{-3}) and

Accepted manuscript

phytoplankton composition. The connected filled circles on the temperature and salinity panels represent the mixed layer depth, calculated as the depth at which the density equals the surface density + 0.03 kg m^{-3} (de Boyer Montégut et al., 2004). The connected filled diamonds on the chlorophyll panel represent the depth at which nitrate reaches 1 µM, a proxy for the nitracline depth. Phytoplankton composition is described as a percentage of picoplankton (< 3 µm, black), nanoplankton (3 µm to 10 µm, blue) and microplankton (> 10 µm, red) biomass; orange symbols represent the ratio of *Prochlorococcus* cells to total picoplankton cells (in % abundance); the dots represent the average value of the top 50 m and the crosses represent the average value of the 50-130 m layer.

Figure 5: Box plots of the distribution of *in situ* (In situ) primary production and satellite-derived (VGPM) primary production recorded at the points where *in situ* production measurements were performed (Sat.) and along the cruise track (Sat. full). Estimates are given for the cool (Nectalis1) and the hot season (Nectalis2). The boxplots denote mean values and 25% and 75% interquartiles (IQ25 and IQ75 respectively); the whiskers represent IQ25-1.5x(IQ75-IQ25) and IQ75+1.5x(IQ75-IQ25); dots represent outliers.

Figure 6: Day (plain line) and night (dashed line) 0-600 m mean vertical profiles of zooplankton wet weight (mg m^{-3}) and mean vertical profiles of 38kHz EK60 scattering volume (dB) during the cool season (Nectalis1, thick line) and the hot season (Nectalis2, thin line).

Figure 7: Estimates of zooplankton and micronekton biomass during the day (D) and night (N) during the cool season (Nectalis1, 1) and the hot season (Nectalis2, 2) using the different methods employed during the cruises. From left to right: distributions of mean S-ADCP Sv (dB) across 0-150 m, mean TAPS biovolume (mg m^{-3}) across 0-200 m, mean zooplankton dry weight (DW, mg m^{-3}) across 0-200 m, mean zooplankton wet weight (WW, mg m^{-3}) across 0-200 m, micronekton wet weight (mg m^{-3}) from cumulated net samplings at discrete depths between 14 and 540 m, mean 38 kHz EK60 Sv (dB) across 0-350 m, and corresponding depth-averaged mean (epi- and mesopelagic layers) of micronecton biomass estimates from the SEAPODYM model. The boxplots denote mean values and 25% and 75% interquartiles (IQ25 and IQ75 respectively); the whiskers represent IQ25-1.5x(IQ75-IQ25) and

Accepted manuscript

ACCEPTED MANUSCRIPT

IQ75+1.5x(IQ75-IQ25); dots represent outliers. Note that biomass estimates from SEAPODYM and EK 60, have been identically averaged over three euphotic depths (~350 m) and day/time periods (see text for further details).

Figure 8. Spatial distribution of the epi- and mesopelagic micronecton biomass (mg m^{-3}) estimated from SEAPODYM at the stations and periods of the cruises (top panels) and the corresponding observed 38 kHz Sv from the EK60 echosounder (bottom) during the cool season (Nectalis1, left panel) and the hot season (Nectalis2, right panel). The day/night signal was removed from the data (see text for details). For the sake of clarity the EK 60 Sv data were arbitrarily re-transformed into a linear scale by computing $10^{-Sv/100}$, but the unit by itself has no significance. The EK 60 data have been vertically averaged over the same depths as the micronekton model incorporated into SEAPODYM (3 euphotic layers ~350 m) and the data was resampled onto the model ¼° grid resolution.

Figure 9: Satellite primary production (VGPM in mgC m^{-2} day^{-1}) and euphotic layer currents from GLORYS (top panel). Averaged micronekton biomass (mg m^{-3}) estimated by SEAPODYM and averaged currents from GLORYS across the water column (0 – 1000m) (bottom panel). Cool season (Nectalis1, left panel), hot season (Nectalis2, right panel).

Accepted manuscript

ACCEPTED MANUSCRIPT

Figure 1

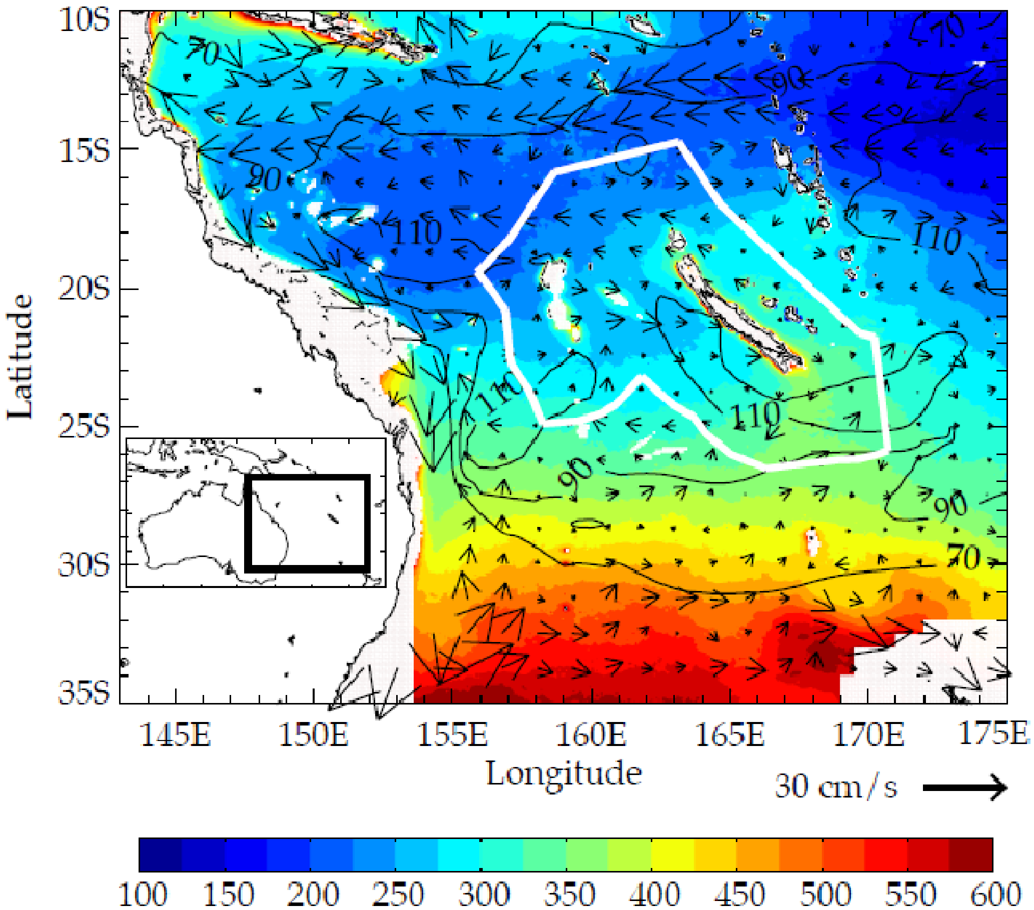

Accept

1432 **Figure 2**

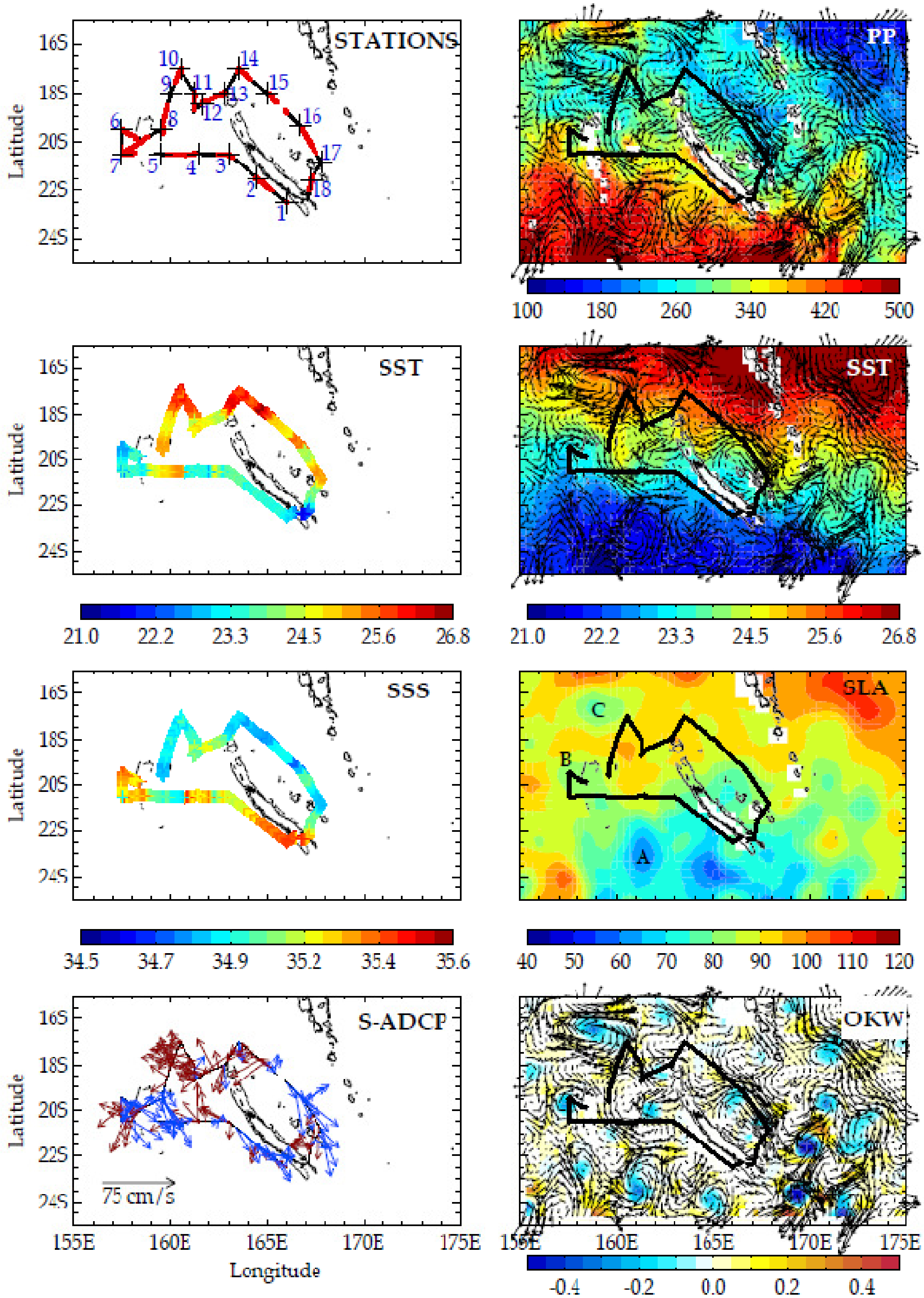

1433

1434

1435 **Figure 3**

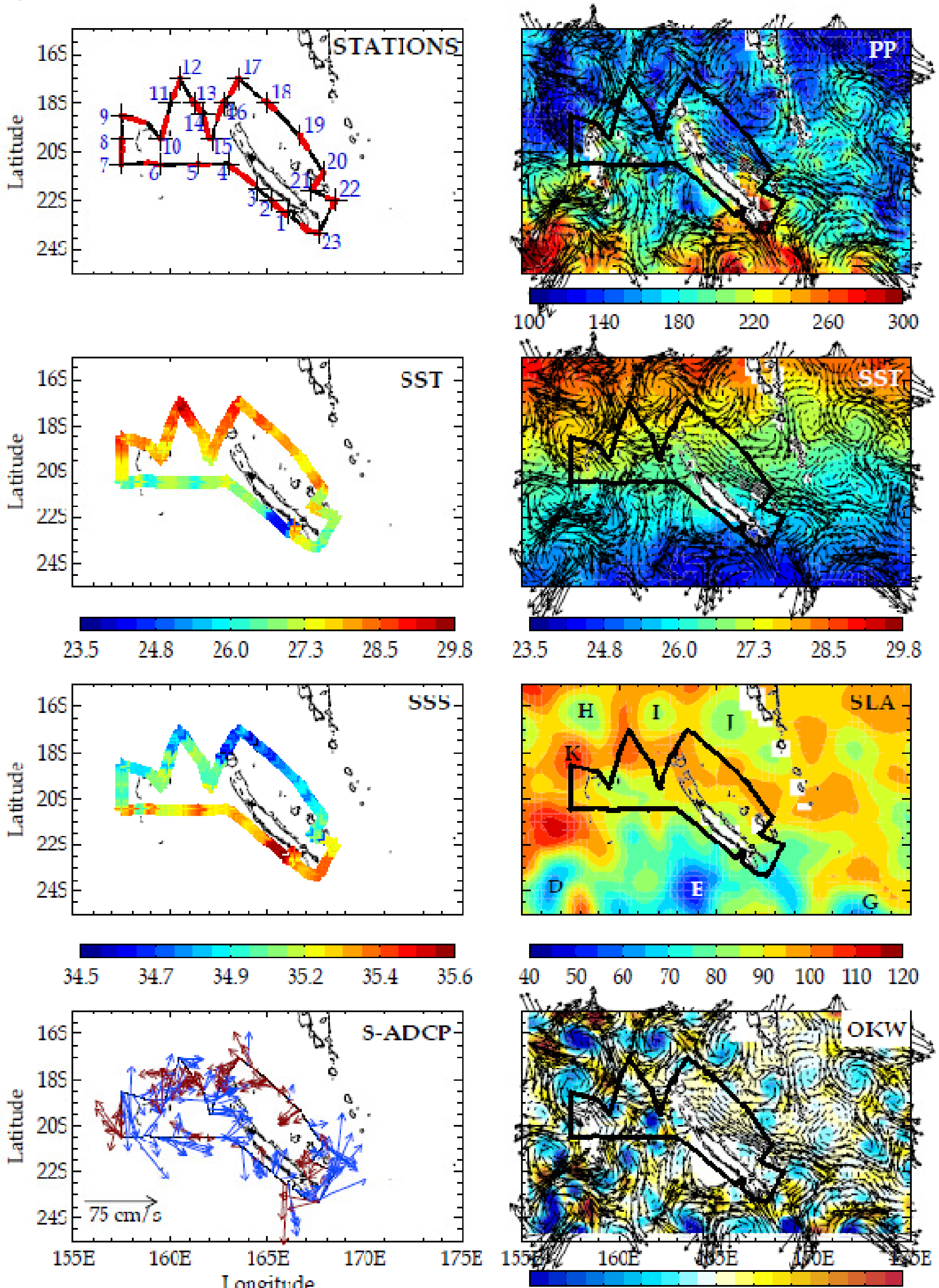

1436

Figure 4

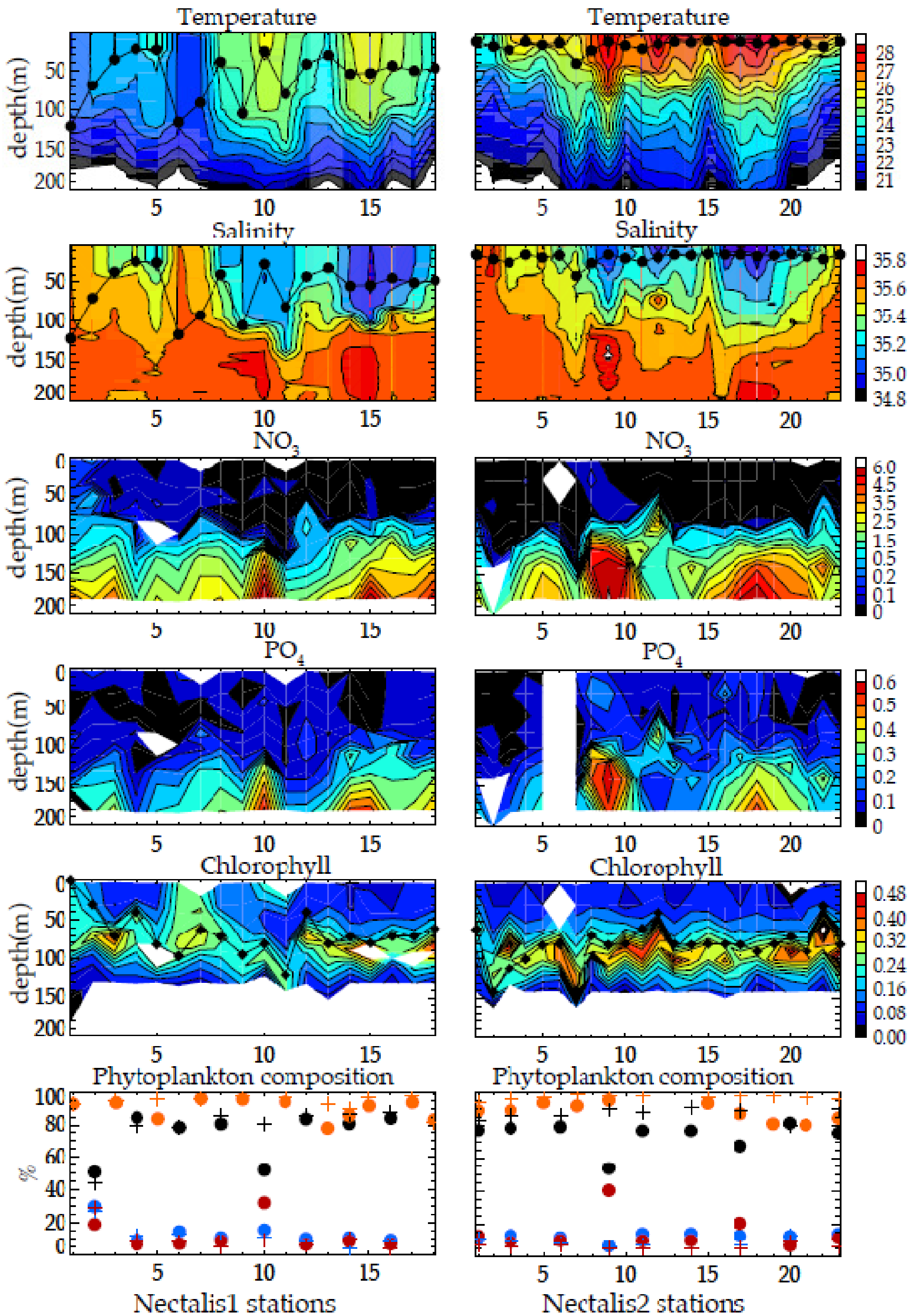
Temperature
Temperature
depth(m)
Salinity
Salinity
NO3
NO3
PO4
PO4
Chlorophyll
Chlorophyll
Phytoplankton composition
Phytoplankton composition
%
Nectalis1 stations
Nectalis2 stations

Figure 5

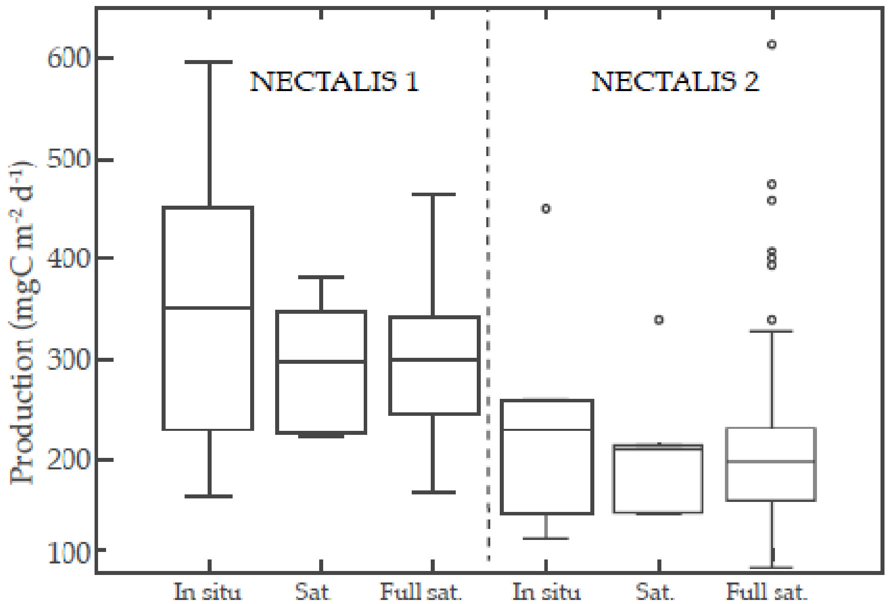

Accepted manuscript

ACCEPTED MANUSCRIPT

Figure 6

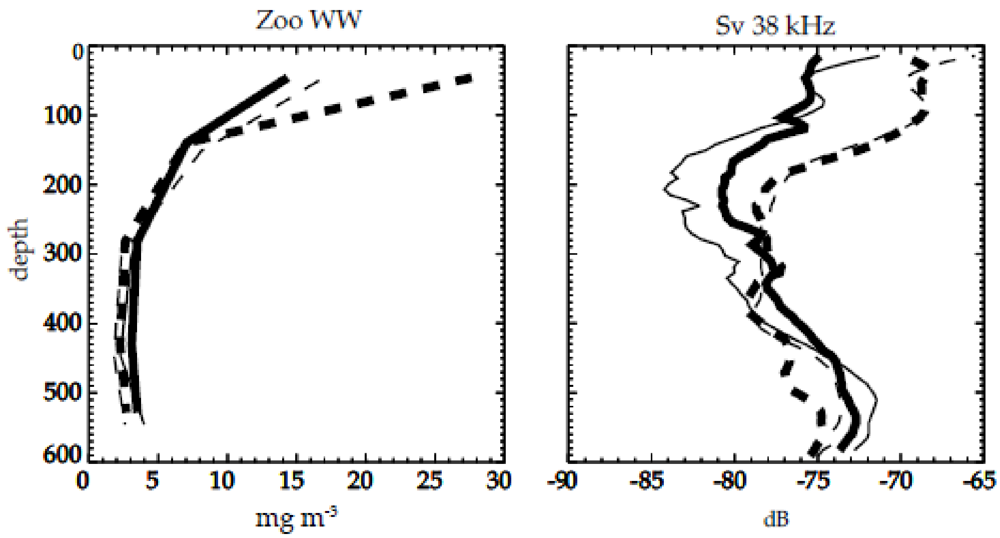

Accepted manu

Figure 7

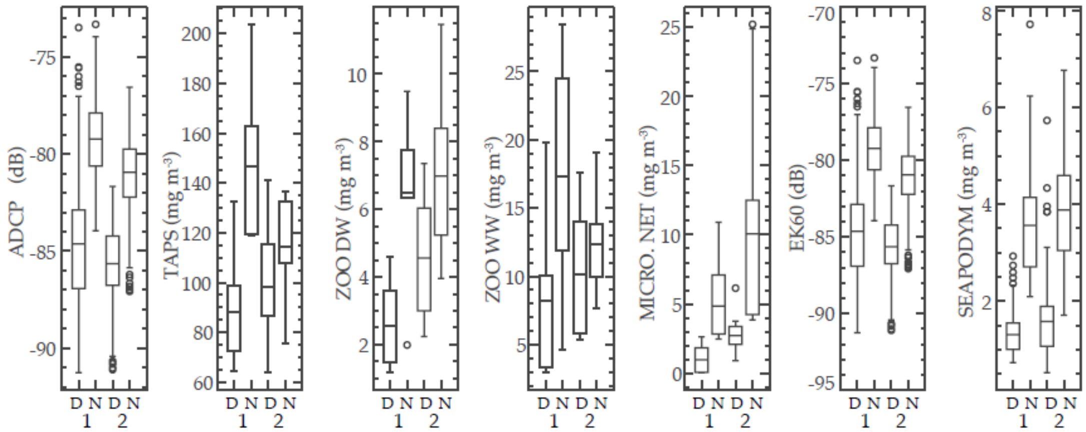

Accepted manuscript

ACCEPTED MANUSCRIPT

1451 **Figure 8**

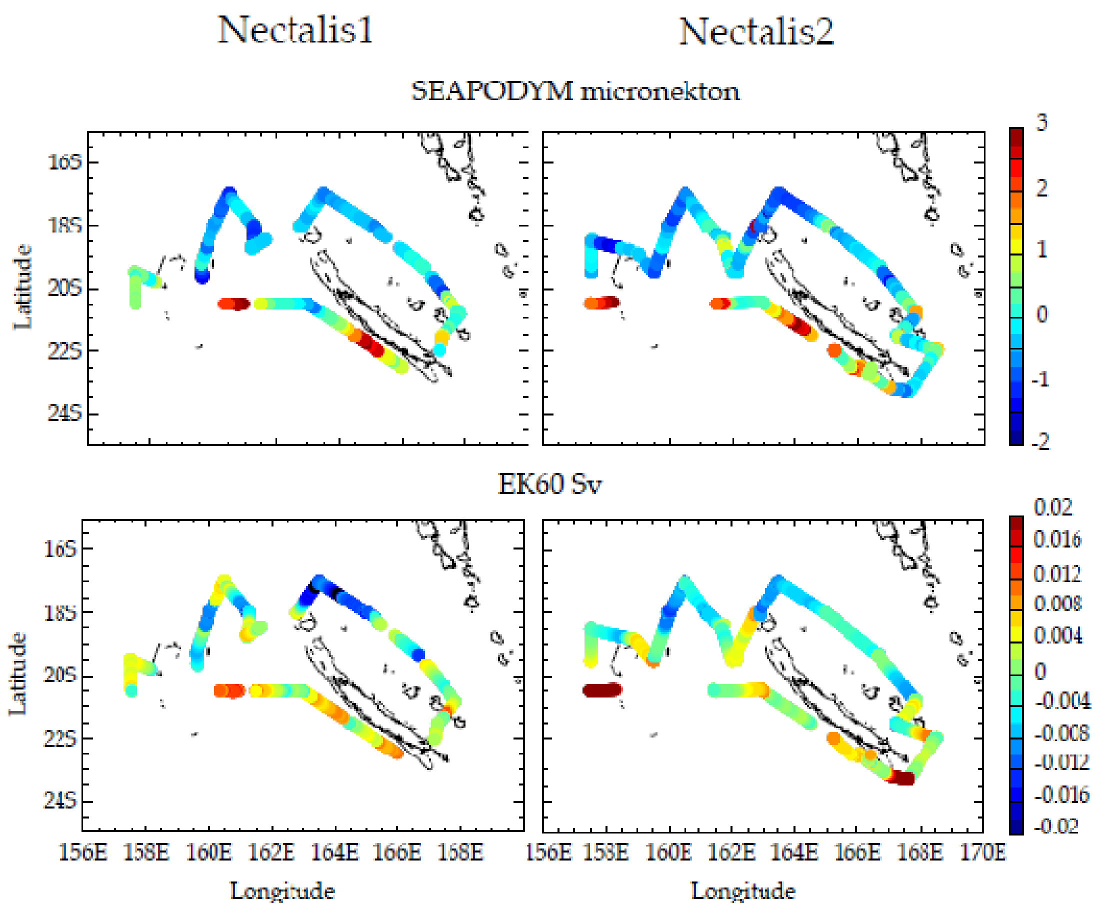

1452

1453

Accepted

ACCEPTED MANUSCRIPT

1454 **Figure 9**

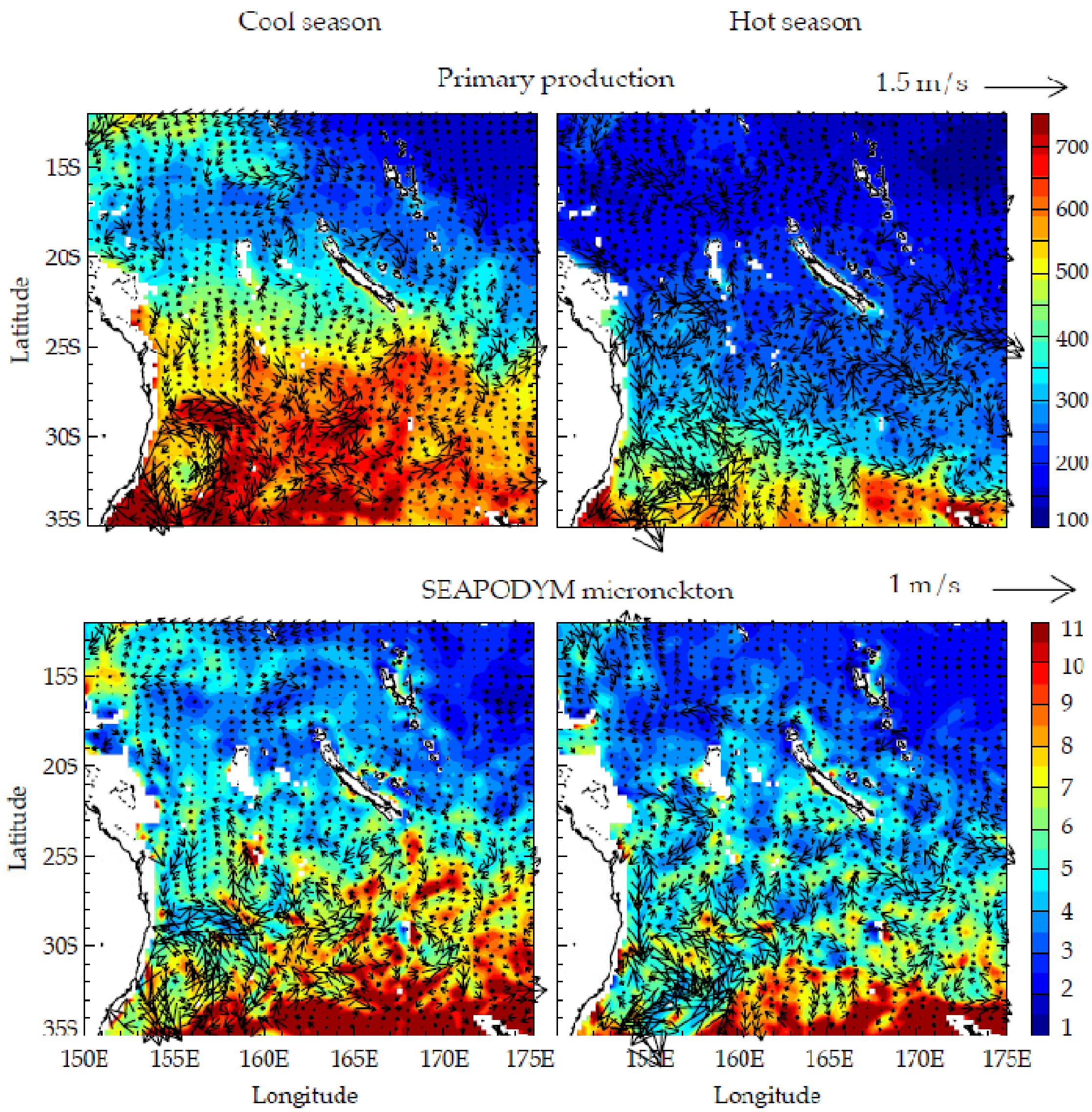

1455